To the Graduate Council:

I am submitting herewith a thesis written by Thomas P. Blanchard, Jr., entitled "Electrochemical Studies of Calcium Chloride-Based Molten Salt Systems." I have examined the final copy of this thesis for form and content and recommend that it be accepted in partial fulfillment of the requirements for the degree of Master of Science, with a major in Chemistry.

Gleb Mamantov, Major Professor

We have read this thesis
and recommend its acceptance:

Accepted for the Council:

Associate Vice Chancellor
and Dean of The Graduate School

ELECTROCHEMICAL STUDIES OF CALCIUM CHLORIDE-BASED MOLTEN SALT SYSTEMS

A Thesis

Presented for the

Master of Science Degree

The University of Tennessee, Knoxville

Thomas P. Blanchard, Jr.

December 1992

For their moral and financial support, the author dedicates this work to his parents Thomas and Elaine Blanchard.

ACKNOWLEDGEMENT

The author would like to express his thanks and sincere gratitude to the following people and organizations:

-Professor Gleb Mamantov for his patience and guidance throughout my graduate studies at the University of Tennessee;

-Drs. W. Bull and E. Wehry, for serving on the authors committee;

-The University of Tennessee Department of Chemistry, The Science Alliance, and Los Alamos National Laboratory for financial support;

-Karl Sienerth and Ellen (Kurt) Hondrogiannis for their assistance in and out of the laboratory;

-To all his friends and relatives for their encouragement;

-Elder Mellon and Author Pratt, for their invaluable assistance with the construction of glassware;

- Anna Mabile for her assistance in undergraduate school.

ABSTRACT

Conductance and EMF studies of $CaCl_2$-based melts were performed in the temperature range 790°C - 990°C. Conductivity data collected using magnesia tubes and capillaries showed deviations from the data recommended by the National Bureau of Standards. These deviations are attributed to the slow dissolution of magnesia by the $CaCl_2$-CaO melt. Conductivity data for molten $CaCl_2$ using a pyrolytic boron nitride capillary were in reasonable agreement with the recommended data; however, undissolved CaO in $CaCl_2$ may have caused blockage of the pyrolytic boron nitride capillary, resulting in fluctuations in the measured resistance. The utility of the AgCl/Ag reference electrode in $CaCl_2$-AgCl and $CaCl_2$-CaO-AgCl melts, using asbestos diaphragms and Vycor glass as reference half-cell membranes, was also investigated. Nernstian behavior was observed using both types of reference half-cell membranes in $CaCl_2$-AgCl melts. The AgCl/Ag reference electrode also exhibited Nernstian behavior in $CaCl_2$-CaO-AgCl melts using a Vycor reference half-cell membrane and a magnesia crucible.

TABLE OF CONTENTS

CHAPTER			PAGE
1.	INTRODUCTION		1
	A.	Review of Relevant Fundamental Properties	5
		1. Electrical Conductance	5
		2. AC Impedance Technique	7
		3. Potentiometry	10
	B.	Review of Literature	14
		1. Electrical Conductance	14
		a. Molten $CaCl_2$	14
		b. Calcium Chloride Binary and Ternary Systems	16
		c. Molten CaO	17
		d. Calcium Oxide Binary and Ternary Systems	17
		2. Conductance Cell Design	18
		3. Potentiometry	20
		a. Cl_2/Cl^- Reference Electrode	21
		b. Ag(I)/Ag Reference Electrode	21
		c. Other Reference Electrodes	22
		d. Reference Cell Membranes	22
	C.	Proposed Research	24
2.	EXPERIMENTAL		26
	A.	Materials	26

CHAPTER PAGE

B. Apparatus 29

1. Dry Box and Vacuum Line 29

2. Furnace Assembly 30

3. Cell Assembly 31

4. Conductance Measuring Equipment 33

5. EMF Measuring Equipment 36

C. Procedure 42

1. Cleaning Procedures 42

2. Conductance Measurements 42

3. Potentiometry 45

3. RESULTS AND DISCUSSION: CONDUCTANCE MEASUREMENTS OF $CaCl_2$-CaO MELTS 47

A. Introduction 47

B. Conductivity Measurements Using MgO Tubes . . 48

C. Conductivity Measurements Using MgO Capillaries 68

D. Conductivity Measurements Using Pyrolytic Boron Nitride 71

E. Other Materials Investigated 78

4. RESULTS AND DISCUSSION: ELECTROMOTIVE FORCE MEASUREMENTS OF $CaCl_2$-CaO MELTS 79

A. Selection of A Reference Electrode 79

B. Selection of A Reference Membrane 81

C. EMF Measurements 82

CHAPTER **PAGE**

1. $CaCl_2$-AgCl System 82

2. $CaCl_2$-CaO-AgCl System 88

5. SUMMARY 99

LIST OF REFERENCES 101

VITA 109

LIST OF TABLES

TABLE		Page
1.	Frequency dispersion of the resistance of molten $CaCl_2$ at 800°C using MgO tubes (data taken from Ref. 91)	51
2.	Specific conductivity data for a $CaCl_2$-CaO melt at 30 kHz: Experiment #1	58
3.	Specific conductivity data for a $CaCl_2$-CaO melt at 30 kHz: Experiment #2	59
4.	Specific conductivity data for a $CaCl_2$-CaO melt at 30 kHz: Experiment #3	60
5.	Activation energy (kcal/mole) for the $CaCl_2$-CaO system	66
6.	Specific conductivity data for a $CaCl_2$ melt at 30 kHz using MgO capillaries	70
7.	Specific conductivity data for a $CaCl_2$-CaO (2 mole % CaO) melt at 20 kHz using a pyrolytic boron nitride capillary	75
8.	Specific conductivity data for a $CaCl_2$ melt at 30 kHz using a pyrolytic boron nitride capillary	77
9.	Summary of emf data for a $CaCl_2$-AgCl melt at 780°C using an asbestos reference half-cell membrane	84
10.	Summary of emf data for a $CaCl_2$-AgCl melt at 810°C using a Vycor reference half-cell membrane	87
11.	Summary of emf data for a $CaCl_2$-CaO-AgCl melt at 820°C using a Vycor reference half-cell membrane and a glassy carbon crucible	93
12.	Summary of emf data for a $CaCl_2$-CaO-AgCl melt at 820°C using a Vycor reference half-cell membrane and a MgO crucible: Experiment #1	95
13.	Summary of emf data for a $CaCl_2$-CaO-AgCl melt at 820°C using a Vycor reference half-cell membrane and a MgO crucible: Experiment #2	96

LIST OF FIGURES

FIGURE		PAGE
1.	Phase diagram for the $CaCl_2$-CaO system	4
2.	Simplified circuit diagram for a Wheatstone bridge	8
3.	Quartz fritted purification vessel	27
4.	Gas flow apparatus	28
5.	Conductance cell assembly	32
6.	Feeding tube apparatus	34
7.	Apparatus used for the transfer of hygroscopic salts	35
8.	Electrode assembly used to support the pyrolytic boron nitride capillary	37
9.	Electrode sealed in MgO or quartz tubing	38
10.	Reference half-cell with an asbestos diaphragm	40
11.	Reference half-cell with a Vycor membrane	41
12.	Frequency dispersion of the resistance of molten $CaCl_2$ at 800°C using magnesia sheathing tubes (data taken from Ref. 91)	49
13.	Plot of measured resistance versus frequency for molten $CaCl_2$ at 800°C using magnesia sheathing tubes (data taken from Ref. 91)	50
14.	Conductance isotherms for molten $CaCl_2$-CaO using magnesia sheathing tubes (data taken from Ref. 91)	52
15.	Activation energy versus CaO concentration (data taken from Ref. 91)	54
16.	Conductance isotherms for the $CaCl_2$-CaO system using MgO sheathing tubes: Experiment #1	55
17.	Conductance isotherms for the $CaCl_2$-CaO system using MgO sheathing tubes: Experiment #2	56

FIGURE PAGE

18. Conductance isotherms for the $CaCl_2$-CaO system using MgO sheathing tubes: Experiment #3 57

19. Specific conductivity of molten $CaCl_2$: (A) data from Figure 18; (B) data from Figure 16; (C) data from Figure 17; (D) data from Figure 14 (Ref. 91); (E) recommended data 61

20. Variation of the cell constant using magnesia sheathing tubes 63

21. Arrhenius plots for the $CaCl_2$-CaO (0 - 14 mole percent CaO) system using magnesia sheathing tubes:(A) data from Figure 18; (B) data from Figure 16; (C) data from Figure 17; (D) recommended data (ref. 48) 64

22. Activation energy for molten $CaCl_2$-CaO using magnesia sheathing tubes: (A) data from Figure 18; (B) data from Figure 16; (C) data from Figure 17 65

23. Specific conductivity data of molten $CaCl_2$: (A) data set #3; (B) data set #1; (C) data set #2; (D) recommended data (ref. 48) . . 67

24. Specific conductivity data of molten $CaCl_2$ using magnesia capillaries: (A) and (B) two sets of measurements; (C) recommended data (ref. 48) . . . 69

25. Frequency dispersion of the resistance of molten $CaCl_2$ at 800°C using a pyrolytic boron nitride capillary 72

26. Specific conductivity data of: (A) recommended data for $CaCl_2$ (ref. 48); (B) molten $CaCl_2$; (C) molten $CaCl_2$-CaO (2 mole percent CaO) 73

27. Specific conductivity data for molten $CaCl_2$: (A) recommended data (ref. 48); (B) measurements using a pyrolytic boron nitride capillary 76

28. Sample half-cell electrode assembly 80

29. Nernst plot for a $CaCl_2$-AgCl melt using an asbestos reference half-cell membrane at 780°C: (A) calculated line; (B) measured data 83

FIGURE **PAGE**

30. Nernst plot for a $CaCl_2$-AgCl melt at 810°C using a Vycor reference half-cell membrane: (A) calculated line; (B) measured data 86

31. Variation of the emf with temperature for a $CaCl_2$-AgCl (0.08 mole fraction) melt using a Vycor reference half-cell membrane: (A) calculated line; (B) measured data 89

32. Nernst plot for a $CaCl_2$-CaO-AgCl melt at 820°C using a Vycor reference half-cell membrane: (A) calculated line; (B) measured data 91

33. Nernst plot for $CaCl_2$-CaO-AgCl melts at 820°C using a Vycor reference half-cell membrane: (A) experiment #1 using a MgO crucible (▲); (B) experiment #2 using a MgO crucible (□); (C) calculated line 97

CHAPTER 1

INTRODUCTION

Interest in the study of molten salts as solvent systems has grown to a considerable extent in recent years. Many aspects of molten salts have been reviewed (1-14). Molten salts are useful as solvent systems since they generally possess high conductivities, low vapor pressures, large decomposition potentials, and are liquid over a wide temperature range. Molten salt solvent systems are especially useful in electrochemical processes where the elimination of water based solutions may be a necessity (15). There are several disadvantages of molten salts, which make their use very difficult. Some salts are very hygroscopic, and must be stored and handled within a dry box, and kept under inert atmosphere outside of the dry box. Some molten salts require high temperatures (> 600°C) to achieve the molten state, and may not be compatible with readily available materials (16). Molten salts have found considerable use as solvent systems in the deposition of some transition metals (17,18), and in the purification of some actinide metals (19).

The use of $CaCl_2$ as a solvent is of interest to Los Alamos National Laboratory (LANL), since it is used in the plutonium metal purification process (19). Plutonium metal

was initially produced by the metallothermic reduction of PuF_4 with Ba metal in the early 1940's (19). Barium metal was later replaced by Ca metal as the reductant for PuF_4 (20).

The PuF_4 reduction is currently being replaced by the direct reduction of PuO_2, due to personnel exposure to neutrons resulting from the (α,n) reaction in fluorine nuclei, and the difficulty in the preparation of anhydrous plutonium fluoride by treatment of the corresponding oxide with HF gas. This direct reduction of plutonium oxide (Direct Oxide Reduction (DOR) method) involves the reduction of PuO_2 with calcium metal in a $CaCl_2$ flux (21). Calcium metal is also widely used in the commercial production of several other actinide metals (19).

The following reaction has been proposed for the reduction of PuO_2 by Ca metal in a $CaCl_2$ solvent (20)

$$PuO_2(s) + 2Ca(l) \longrightarrow 2CaO(l) + Pu(l)$$

The $CaCl_2$ serves to dissolve the CaO byproduct permitting coalescence of molten plutonium metal (20). Essentially no purification of the plutonium metal takes place in the DOR process, implying that the purity of the plutonium metal is on the order of the purity of the plutonia feed stock. Advantages of the DOR method have been reported (20). Molten $CaCl_2$ is well suited for a molten salt bath, since

the solubility of CaO in $CaCl_2$ is 18.5 mole % at 830°C (Figure 1) (22), and plutonium metal is insoluble in a $CaCl_2$-Ca-CaO melt (23). A review of the function of $CaCl_2$ in the reduction of PuO_2 has been reported (24).

The DOR method results in the production of impure plutonium metal, and further purification of the impure metal is required. The electrorefining method (ER) is one method used at LANL to further purify the impure Pu metal; it results in a plutonium metal purity of > 99.9 % (20). Several methods, including the ER method, for the purification of actinide metals have been reviewed (20,23).

Calcium chloride-based molten salt systems have been used in various other commercial applications. Sharma and Seefurth (25) described a process for the production of a low-cost Nd metal used in the production of Nd-Fe alloys for the manufacture of permanent magnets. The process involved the reduction of neodymium oxide (Nd_2O_3) by calcium metal in a $CaCl_2$-NaCl melt. Calcium chloride has also been used in the production of Al-Cd alloys (26). Besides the production of alloys, $CaCl_2$-based systems have also been employed in the production of sodium (27), magnesium (28), and calcium metals (29).

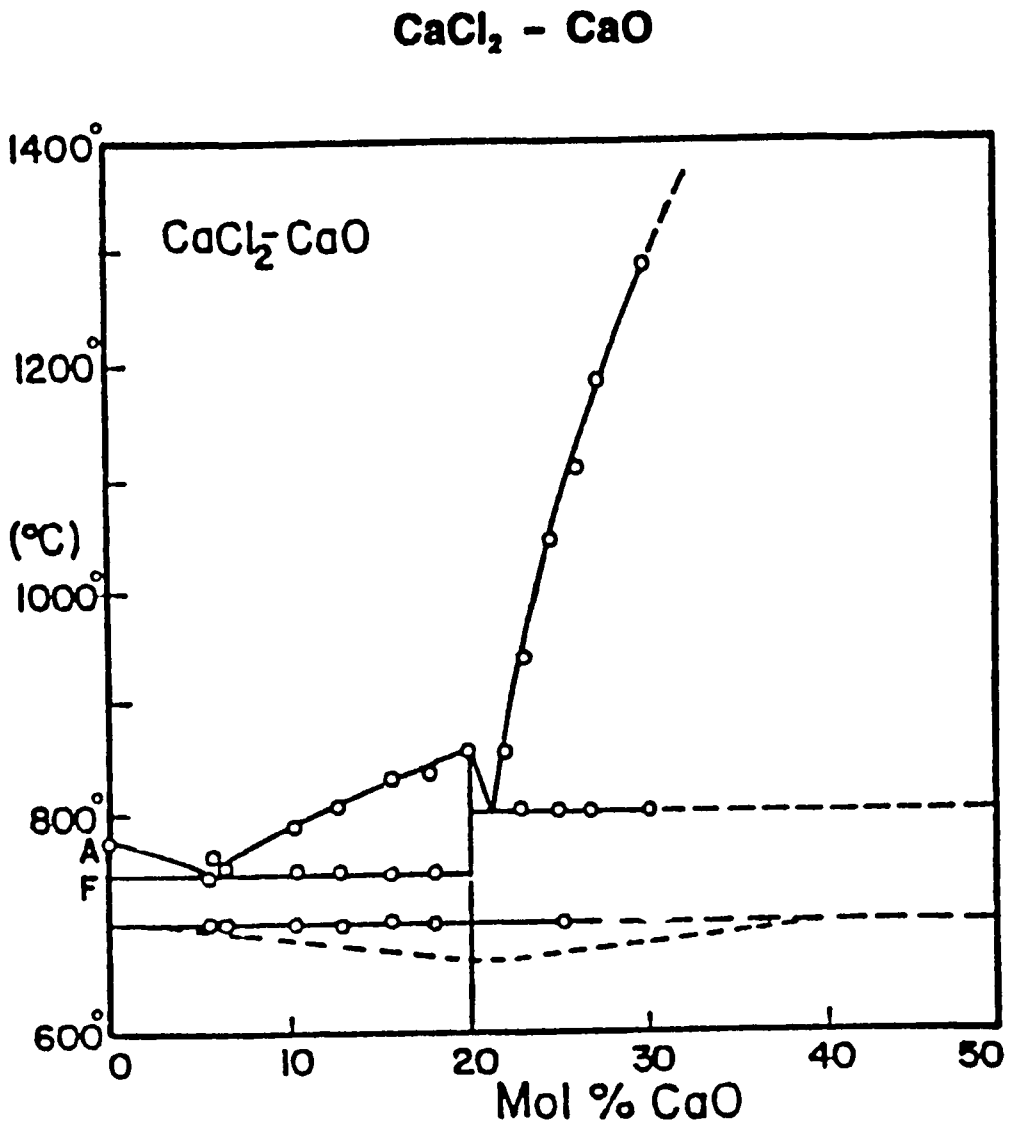


Figure 1. Phase diagram for the $CaCl_2$-CaO system.

A. Review of Relevant Fundamental Properties

1. Electrical Conductance

The study of the electrical conductance of molten salts is of fundamental importance for the understanding of ion transport properties in molten salts. Other properties, such as ion mobility and complex formation, may be understood through the measurement of the electrical conductance. The conductance, L, of a solution is the inverse of its resistance

$$L = 1/R \tag{1}$$

where R is the resistance between two electrodes immersed in a solution. For electrodes with a cross sectional area, A (cm^2), separated a distance, l (cm),

$$R = \rho(l/A) = 1/\kappa(l/A) \tag{2}$$

where R is the solution resistance, ρ(ohm-cm) is the specific resistivity, κ (S/cm) is the specific conductivity, and l/A (cm^{-1}) is the cell constant, which is a characteristic of the cell. The term l/A is usually determined by measuring the resistance of standard solutions, whose conductivities have been thoroughly investigated and proven to be reliable (30, 31). Such

solutions were reported by Jones and Bradshaw (30), who adopted the demal concentration scale in the determination of the conductance of 0.01, 0.1 and 1 demal KCl solutions. The demal concentration scale (equivalents/dm^3) was proposed by Parker and Parker (32). An alternative method, which allowed for the absolute determination of the cell constant, has been reported by Saulnier (33,34). A review of the assessment of the practices used in the determination of the cell constant is provided by Janz and Tomkins (35).

For systems with high specific conductivities, as for many molten salts, the measured resistances can be too low for accurate measurements to be made with conventional instrumentation. In those cases, capillary type cells are often employed, which results in an increase in the cell constant. Capillaries must be constructed of insulating materials to prevent electrical shorts in the conducting path, and must be compatible with the melt system. Compatibility is an important issue, since the magnitude of the measured resistance is largely determined by the diameter of the capillary, and changes in its diameter can cause significant changes in the measured resistances. Errors in the data will result if the cell constant is allowed to change while conductance measurements are in progress. Some types of capillary materials for use in molten salts have been reviewed by Robbins (36).

The activation energy for the conduction may be obtained using the Arrhenius equation

$$\kappa = A\ e^{-Ea/RT} \qquad (3)$$

where A is a constant, E_a (kcal/mole) is the activation energy for conduction, R is the molar gas constant, and T is the temperature in Kelvin. The activation energy for conduct-ion can be obtained by determining the slope of a plot of ln (κ) vs. 1/T (K). The temperature dependence of the conductance of molten salts has been studied by Matiasovsky et al. (37).

2. AC Impedance Technique

The ac impedance technique is one of the most common techniques used for the measurement of the electrical conductance. This technique often employs some form of the basic Wheatstone bridge circuit. A basic Wheatstone bridge design (38) consists of two matched resistors, R_{std}, in the upper arms, with the cell and an external variable resistor (R) and variable capacitor (C), usually connected in parallel, in the lower arms (Figure 2). An ac signal is applied across the cell, and is detected using a phase sensitive null detector (usually an oscilloscope). An ac current is used in conductance measurements to minimize polarization effects (39). Cell parameters such as the

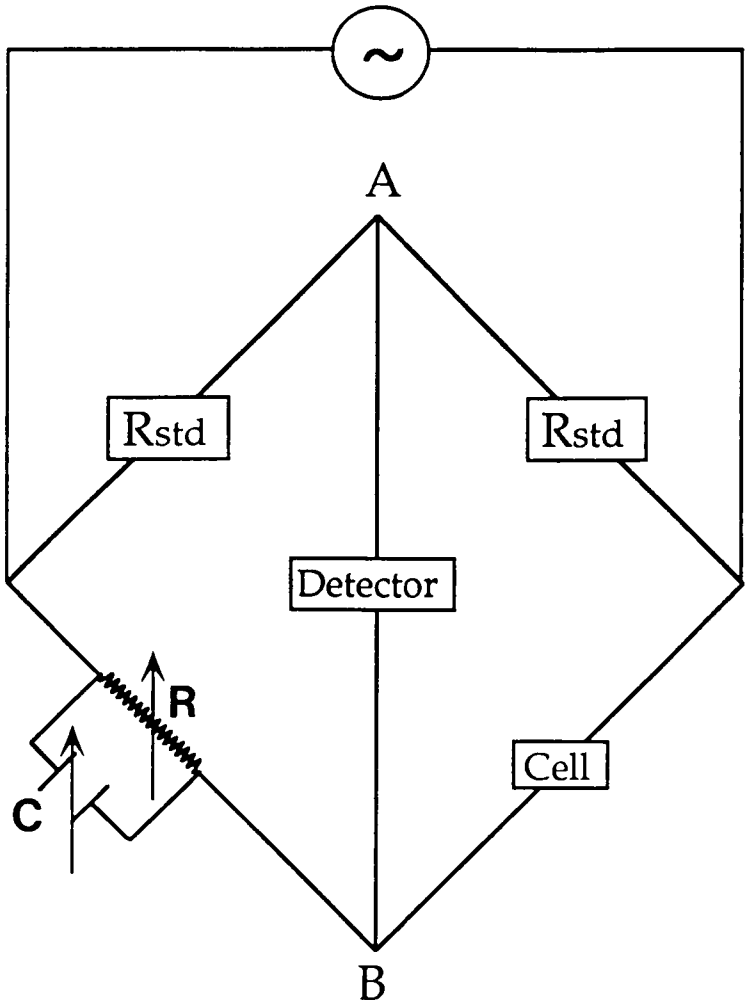


Figure 2. Simplified circuit diagram for a Wheatstone bridge.

double layer capacitance and the faradaic impedance are in series with the solution resistance, and are usually balanced using a parallel RC combination (39), since balancing smaller capacitances is more accurate than balancing large capacitances, and since handling large variable capacitors may be quite cumbersome. When balancing a series RC combination with a parallel RC combination, the measured resistance will have some dependence upon the applied frequency (i.e., will show a frequency dispersion) (40), and must be calculated using the equation

$$R_s = R_b / (1 + (\omega R_b C)^2) \qquad (4)$$

where

R_s = the solution resistance

R_b = the measured resistance

ω = the angular frequency (rads/cm)

C = the measured capacitance.

Since balancing a series RC combination with a parallel RC combination shows a frequency dispersion, there will be a dependence of the measured resistance on the frequency, and extrapolation to infinite frequency as a function of $\omega^{1/2}$ may be necessary (40, 41).

The variation of the measured resistance with frequency has been described by Jones and Christian (42), Ives and

coworkers (43), and Janz and coworkers (44). It is important that the amplitude of the applied ac voltage be sufficiently low that electrochemical reactions with the melt and the electrodes are eliminated. In most of this work an applied voltage of 30 mV was used; lower applied voltages were observed to decrease the sensitivity of the measurement. Polarization resistance can also be minimized by platinizing the electrodes (45). Platinized electrodes have been used at elevated temperatures in molten salts (46). However, the measured resistances were observed to drift slowly, due to the loss of the platinum black at the high temperatures. In this work, platinized electrodes were not used, due to the high temperatures (800°C - 1000°C), and the corrosiveness of the CaO-containing melts.

3. Potentiometry

Potentiometry has been used extensively in molten salts for the determination of the electromotive force (emf) series in a variety of molten salt systems. Electromotive force measurements are very valuable for the determination of thermodynamic properties of molten salts, as well as studies of complex formation, decomposition potentials, free energies, and the stability of various solute species.

One criterion for the reversibility of a redox couple (Ox/Red) in the general reaction

$$Ox + ne^- \rightleftharpoons Red \quad (5)$$

is that it follows the Nernst equation

$$E_{eq} = (E^\circ_{O/R}) + RT/nF \ln a_{ox}/a_{red} \quad (6)$$

where

E_{eq} = equilibrium potential, volts (V)

$E^\circ_{O/R}$ = standard potential of the electrode couple, V

R = molar gas constant (8.315 Joules $mole^{-1}$ $degree^{-1}$)

T = absolute temperature

F = Faraday constant (96,487 coulombs)

n = number of electrons transferred

a_{ox} = activity of the oxidized form

a_{red} = activity of the reduced form.

If a standard state is chosen such that the activity coefficient of the solute species approaches unity as the solution approaches infinite dilution, then it may be assumed that the activity of the ions in solution approximates that of the concentration of the ions, and equation (6) may be written as

$$E_{eq} = (E^\circ_{O/R}) + RT/nF \ln [C_{ox}]/[C_{red}] \quad (7)$$

If the reduced form, Red, is the metallic state, the equilibrium potential may be expressed as

$$E_{eq} = (E^{\circ}_{O/R}) + RT/nF \ln [M^{n+}] \quad (8)$$

Equilibrium potentials are often measured against a reference electrode in cells of the type

Reference electrode // M^{n+} / M

The resulting cell potential is then given by the expression

$$E_{cell} = (E^{\circ}_{O/R}) + RT/nF \ln [M^{n+}] - E_{ref} \quad (9)$$

where E_{ref} is the potential of the reference half-cell. For cells with the same metal/metal ion couple in both the sample and reference half-cells which are separated by a liquid junction, equation (9) may be stated as

$$E_{cell} = (E^{\circ}_{O/R}) + RT/nF \ln [M^{n+}_s]/[M^{n+}_r] + E_{lj} \quad (10)$$

where

E_{cell} = cell potential

M^{n+}_s = concentration of the metal ion in the sample half-cell

M^{n+}_r = concentration of the metal ion in the reference half-cell

E_{lj} = liquid junction potential.

In cases where essentially the same solutions are used in both compartments, the value of E_{lj} is negligible and can be omitted reducing equation (10) to

$$E_{cell} = (E^\circ_{O/R}) + RT/nF \ln [M^{n+}_s]/[M^{n+}_r] \quad (11)$$

However, for cells employing different solutions, significant junction potentials may exist, and they must be corrected (47). The value of E_{lj} can be determined by measuring the cell potential with the same solution in both compartments. From equation (11), the number of electrons transferred in the Ox/Red reaction (equation (5)) may be evaluated by obtaining the slope of the plot of E_{cell} vs. ln $[M^{n+}_s]/[M^{n+}_r]$. The standard electrode potential ($E^\circ_{O/R}$) for the Ox/Red couple can be determined by extrapolation to $[M^{n+}_s]/[M^{n+}_r] = 1$, provided the E_{lj} is negligible.

There are three most often used expressions for the concentration scale, molality, molarity, and mole fraction. The data reported in this thesis are for the mole fraction scale.

B. Review of Literature

1. Electrical Conductance

The electrical conductance of a molten salt is an important property when considering its use as a solvent system for use in electrochemical processes. The incompatibility of materials (for example, quartz, Vycor, alumina) in CaO-containing melts has presented the experimenter with many difficulties in the design of the conductance cell, and in the determination of the electrical conductivity for the $CaCl_2$-CaO melt system. Conductivity data for $CaCl_2$ and its chloride systems have been reviewed (48). Some of the literature data recommended by Janz and coworkers in a National Bureau of Standards publication (48) for the conductivity of $CaCl_2$, and some of its binary and ternary systems are reported here, along with a brief description of the experimental procedure. A review of the literature data on molten CaO and some of its binary and ternary systems is also included.

a. Molten $CaCl_2$

Bockris et al. (49) measured the conductivity of molten $CaCl_2$ in the temperature range 771°C to 1018°C. Resistances were measured from 500 Hz to 10 kHz, and were extrapolated to infinite frequency. The cell used was similar to the one employed by Van Artsdalen and Yaffe (50) who employed a

quartz dip-type capillary cell with platinum cylindrical electrodes. Cells were calibrated using aqueous 1 demal KCl solutions (35); no mention was made of the magnitudes of the cell constants. The conductivity values calculated for $CaCl_2$ ranged from 1.786 S/cm at 771°C to 3.096 S/cm at 1018°C. The reported accuracy for the conductance measurements was ± 0.25%. These data have been reported by Janz et al. (48) to be the recommended data for the conductivity of pure salts.

Other investigators have measured the conductivity of molten $CaCl_2$ before measuring the conductivity of $CaCl_2$ binary and ternary systems. Lee and Pearson (51) measured the conductivity of molten $CaCl_2$ in the temperature range of 750°C to 950°C, and an applied frequency of 1 kHz. A quartz capillary cell employed platinum cylindrical electrodes, which were suspended from the top of the cell by platinum wires fastened to bakelite caps, which were made to fit the quartz tubes. Cell constants were determined using normal solutions of KCl at 0°C, and ranged from 775 cm^{-1} to 1100 cm^{-1}. The values obtained ranged from 2.12 S/cm at 800°C to 2.78 S/cm at 950°C. The accuracy of the measurements was reported to be ± 1%.

Grjotheim et al. (52) measured the conductivity of molten $CaCl_2$ in the temperature range 820°C to 900°C. The measured resistances were recorded at various frequencies ranging from 2 kHz to 20 kHz, and were extrapolated to

infinite frequency. The conductance cell was constructed from an Al_2O_3 tube 4 mm I.D. x 13 cm long, and utilized platinum cylindrical electrodes. The cell constant was determined using aqueous 1M KCl solutions at 20°C and was checked with saturated aqueous NaCl solutions at 20°C. The cell constant was on the order of 50 cm^{-1}. The values obtained for pure $CaCl_2$ were 2.093 S/cm at 800°C and 2.465 S/cm at 900°C, which deviated by -1.1 % and -3.7% from the data recommended by Janz et al. (48).

Other authors have measured the conductivity of $CaCl_2$, and have shown larger deviations from the recommended data; they were therefore not included in this summary. An extensive list of conductivity data for single salts has been compiled (53).

b. Calcium Chloride Binary and Ternary Systems

Conductivity data for several binary $CaCl_2$ molten salt systems have been measured. Grjotheim et al. (52) have also measured the conductivity of binary and ternary systems of $CaCl_2$, $MgCl_2$, and KCl. Recently, Iwadate et al. reported conductivity data for the $PrCl_3$-$CaCl_2$ (54), $NbCl_3$-$CaCl_2$ (55), and the $LaCl_3$-$CaCl_2$ (56) systems. A more extensive list of the conductivity of binary mixtures consisting of $CaCl_2$ and other salts has been summarized by Janz et al. (57, 58).

Lee and Pearson (51) studied the electrical conductivity of the four component system consisting of $CaCl_2$, $MgCl_2$, KCl, and NaCl salts.

c. Molten CaO

The conductance of molten CaO has been studied by Tomlinson (59), who obtained one experimental data point at the melting point of CaO. The experiment involved measuring the conductivity of CaO by the production of a pool of molten oxide in the center of a solid block by means of a high intensity electric carbon arc. The resistance between two pools of platinum, produced by fusion of two platinum leads passing through the base of the block, was measured using an ac bridge. The accuracy of the measurement was reported to be no better than ± 50%. Conductivity data for several other molten metal oxides have been measured by Van Arkel *et al*. (60).

d. Calcium Oxide Binary and Ternary Systems

The conductivity of CaO binary melts has been studied by several authors (58). Baak (61,62) has studied the conductivity of CaO-CaF_2 systems, where he observed a maximum in the conductivity of CaF_2 at 6.5 mole % CaO.

Bockris *et al*. (63,64) measured the conductivity of CaO in molten silicates, in the temperature range 1000°C - 1800°C, and a composition range 0.27% - 0.60% CaO in

molten SiO_2. They reported an increase in the conductivity with the increase in the metal oxide. Resistance measurements were made in molybdenum resistance furnaces using a Wheatstone capacitance bridge in the frequency range 500 Hz - 10 kHz; molybdenum rods were used as electrodes. The cell constant was measured with various concentrations of KCl at 25°C.

Martin and Derge (65) investigated the ternary system $CaO-Al_2O_3-SiO_2$ in the temperature range 1400°C - 1620°C, with compositions of 35.15% - 50.1% SiO_2, 5.0% - 19.7% Al_2O_3, and 35.1% - 50.05% CaO. They observed an overall decrease in the conductivity with the decrease in the CaO concentration in the melt system.

2. Conductance Cell Design

The design of a conductance cell is an important aspect in the measurement of the electrical conductance of solutions. Cell designs for conductivity measurements in molten salts have been reviewed (9,66,67). A suitable cell design should allow for a constant electrode separation, a sufficiently large electrode cross sectional area, to reduce polarization effects, and separation of electrical leads, to reduce unwanted capacitance effects across the leads at high measured resistances (40). In molten salt solutions where the conductivity can be on the order of 1 S/cm - 10 S/cm, large cell constants are desired. The experimental approach

is then to employ cells with capillary sheathing material, which can result in a cell constant in the range of a few hundred cm^{-1}. Capillary materials must be constructed from insulating material to prevent electrical shorts, and must be compatible with the system of interest, since minute changes in the diameter of the capillary can cause significant changes in the cell constant. For corrosive systems metallic cells are often employed, in which the container is used as one of the electrodes (36). In the metallic cell design, cell constants on the order of a few tenths cm^{-1} are usually obtained, requiring more accurate measurements of the lead resistance, and in the control of temperature gradients. Also, the cell constant will be dependent upon the amount of solution in the container, and in the position of the other electrode. Experimentally, capillary type cells are desirable for use in most molten salts.

The selection of conductance cell materials should be dependent upon the system of interest, and the maximum operating temperature. Robbins (36) has listed several materials which have been used in the construction of conductance cells used with high temperature molten salts. For molten salts with melting points lower than ca. 550°C, Pyrex capillary cells may be used. Pyrex provides for simple cell construction, since tungsten (often used as a current carrier for platinum electrodes) can be sealed

directly to Pyrex tubing, eliminating the need for cement or Pyrex to quartz graded seals. In molten salts with melting points above ca. 550°C, other materials must be considered. Quartz cells are often employed due to the high melting point of quartz and its low thermal expansion coefficient (68). In more corrosive melts, other materials such as alumina, magnesia, boron nitride, and metals, must be considered for cell construction.

3. Potentiometry

A requirement for the measurement of electrode potentials is a suitable reference electrode. A satisfactory reference electrode should be reversible, stable with time, non-polarizable, and compatible with the melt of interest. The incompatibility of materials with CaO-containing melts has introduced complications in the development of a suitable reference electrode for use in a $CaCl_2$-CaO melt. Reviews are available on a variety of reference electrodes for use in molten salts, including molten chlorides (13,29,47). Electromotive force data for $CaCl_2$-based media are very scarce, and only a few systems have been reported (13,69). The following discussion provides data on several reference electrodes used in molten chloride media.

It has been stated (70) that, "It is unlikely that a universal reference electrode of thermodynamic significance

can be devised for general use in different molten solvents at varied temperatures." Redox couples such as, Cl_2/Cl^-, Ag(I)/Ag, Pt(II)/Pt, and Al(III)/Al are the most often used reference electrodes in molten chlorides. A brief discussion of these reference electrodes is given below.

a. Cl_2/Cl^- Reference Electrode

The chlorine/chloride reference electrode has been used in the determination of electrode potentials in a variety of molten chloride systems (29). Several designs of the chlorine reference electrode have been described (71). Difficulties in the handling of chlorine gas at high temperatures make this reference electrode undesirable for most molten salt systems.

b. Ag(I)/Ag Reference Electrode

One of the most popular metal-metal ion reference electrode used in molten chloride media is the silver chloride/silver reference electrode. The silver chloride/silver reference electrode has been used to measure electrode potentials in a variety of molten chloride salts (29, 71, 72). The potential of the Ag(I)/Ag reference electrode is determined by the half-reaction shown below

$$AgCl(s) + e^- \rightleftharpoons Ag(s) + Cl^-$$

The advantage of this electrode is that it is reversible in a large variety of molten chloride media, it can be employed at temperatures up to ca. 950°C, and its construction is relatively simple. Flengas and Ingraham (73-76) have measured electrode potentials of several metal chloride couples in NaCl-KCl based melts using the AgCl/Ag reference electrode. More recently, Tumidajski and Flengas (77,78) studied the thermodynamic behavior of Cr, Ag, Co, Ni, Fe, and Cu in equimolar mixtures of NaCl, KCl, and CsCl using a Ag(I)/Ag reference electrode between 700°C and 900°C. Yang and Hudson (79) have studied selected metal chlorides in a LiCl-KCl eutectic using a AgCl/Ag reference electrode.

Other melt systems in which the Ag(I)/Ag reference electrode was employed have been reviewed (47, 72).

c. Other Reference Electrodes

Other reference electrodes such as Pt(II)/Pt and the Al(III)/Al have been used in molten chlorides (29,47,71,80).

d. Reference Cell Membranes

Electrode potentials of redox couples are generally measured versus a reference electrode whose potential has been established, or is arbitrarily taken to be zero, and remains constant. For a reference electrode to possess a constant potential, the activity of the metal ion in the reference compartment must remain constant. In most cases,

some type of membrane material is often used to separate the reference solution from the solution under investigation. Several types of reference cell membranes have been used in molten salts.

Laity (47) has presented a review of some reference electrodes, and of the membrane materials used for each reference electrode. Some common reference membranes include Pyrex (79), Vycor (81,82), asbestos diaphragms (83), ZrO_2 (84), porcelain (85), ß-alumina (86), and Jena Supremax glass (87). Pyrex membranes and Jena Supremax glass can only be used at temperatures lower than approximately 600°C, and 800°C, respectively, and therefore were not examined as possible reference membrane materials. Porcelain and ZrO_2 are soluble to some extent in a CaO-containing melt, and could not be employed with the melt system under investigation. Difficulties in the exchange of Na^+ with Ca^{2+} in Na^+ ß-alumina hindered its use in the molten chloride system. The two materials which were investigated were asbestos diaphragms and Vycor glass. Flengas and Ingraham (73,76) employed asbestos plugs in KCl-NaCl melt systems at selected temperatures, and obtained reliable data. The disadvantages of using asbestos plugs are the difficulty and reproducibility of construction, and their leakage upon prolonged periods of use. Of the membrane materials listed, Vycor was best suited for use as a reference membrane in the

melt system studied and the temperature range used. The construction of the Vycor reference electrode is described in Chapter 2.

Proposed Research

The purpose of this research was to perform conductance measurements and emf measurements using a $CaCl_2$-CaO molten salt system. A number of experimental problems had to be addressed in performing these experiments. One of the major problems encountered was the incompatibility of most materials with a $CaCl_2$-CaO melt. Due to the corrosiveness of the melt, very few readily available materials can be used for this system, which also limits the possible cell designs for both the conductivity measurements and the emf measurements. Most of the materials which can be used are not easily machinable, and can only be made into a few basic designs (tubes, crucibles, etc.). Also, most of these materials are quite expensive, and usually require basic designs to be custom made upon request, which may take several months.

Since the ac impedance bridge employed in this work was limited to measuring resistances to ± 0.1 ohm, and the measured resistances were typically in the range 1 to 5 ohms, capillary sheathing materials were needed to increase the cell constant. Even with the capillary sheathing

materials, the cell constant obtained was on the order of 100 cm^{-1} for virgin MgO capillaries, 30 cm^{-1} for virgin MgO tubes, and 50 cm^{-1} for pyrolytic boron nitride capillary. The MgO sheathing materials were observed to be slightly attacked by the melt.

CHAPTER 2

EXPERIMENTAL

A. Materials

Anhydrous calcium chloride (4-8 mesh, Alfa Products) was purified by treatment with semiconductor grade HCl gas (Holston Gases, 99.995%) and pre-purified nitrogen (Holston Gases, 99.998%) (88,89) using a quartz fritted vessel depicted in Figure 3. The upper segment of the vessel was loaded with $CaCl_2$ within the dry box. Segments of Tygon tubing compressed with thumbscrew clamps were employed to temporarily seal the vessel for transfer from the dry box to the gas flow apparatus shown in Figure 4. The gas flow apparatus was used to direct the flow of nitrogen and hydrogen chloride gas through the quartz fritted vessel. The $CaCl_2$ was then vacuum dried at 500°C for at least 24 hours before being purged with an HCl/N_2 mixture (ca. 1:1 ratio) at 800°C for approximately six hours, at which time only nitrogen was allowed to purge through the melt for an additional 30 minutes to remove the HCl gas. The salt was then filtered through the quartz frit and degassed under vacuum for ca. 5 minutes while the temperature was increased to 900°C. After sufficient cooling under vacuum, the lower segment of the quartz fritted vessel was sealed with an

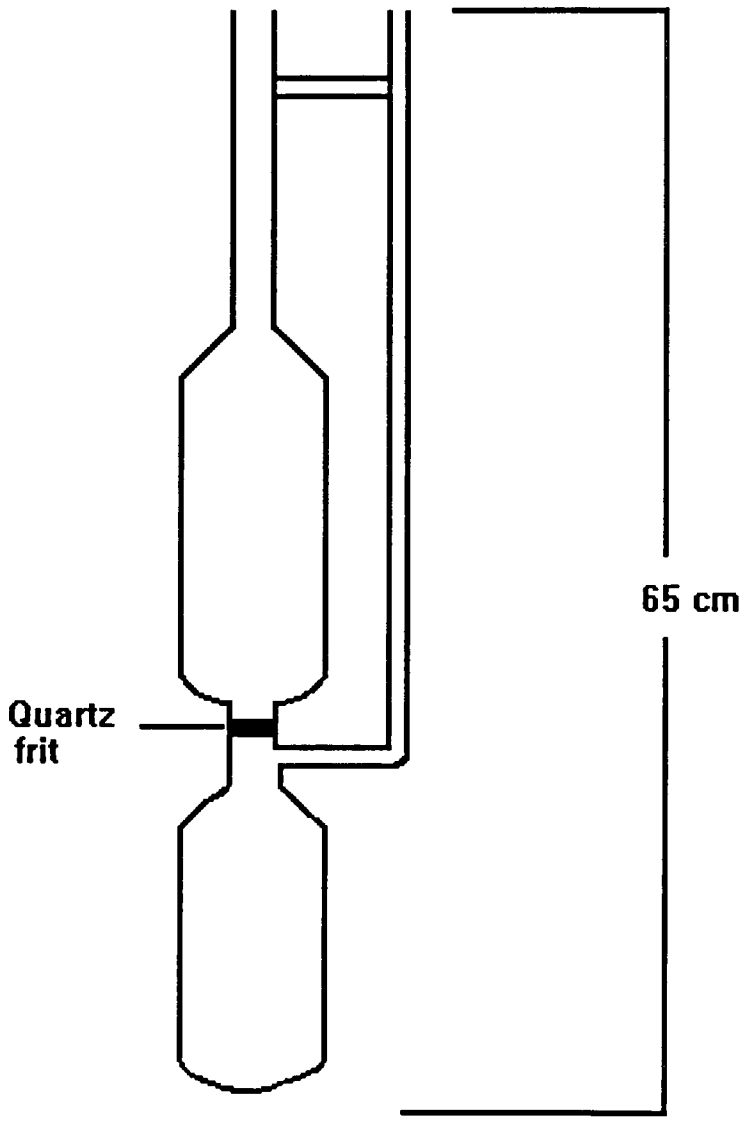


Figure 3. Quartz fritted purification vessel.

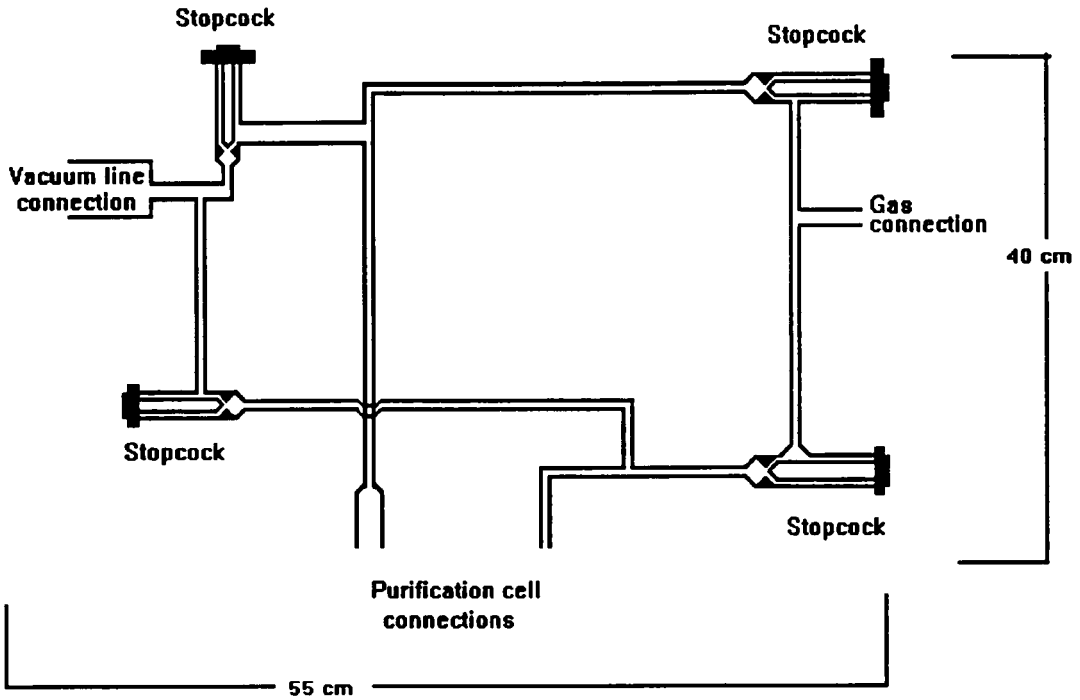


Figure 4. Gas flow apparatus.

oxygen/gas flame, and the resulting purified $CaCl_2$ was stored in the lower segment of the quartz cell.

Calcium oxide (J. T. Baker Co.) was vacuum dried at 900°C for ca. 24 hours in a MgO crucible, and then transferred to the nitrogen filled dry box for storage.

Silver chloride (Aesar Co., 99.99%) was used without further purification. The AgCl was stored inside a dry box, and kept inside an opaque container to minimize photodecomposition.

Sodium chloride and potassium chloride (Mallinckrodt, A.C. S. reagent grade) solutions were used for the calibration of the conductance cell. Both salts were purified by drying under vacuum in Pyrex tubes at 450°C for at least 4 days, and were stored inside a dry box. Distilled water was used in the preparation of all the calibration solutions. Molten KCl and molten NaCl were used for the calibration of the conductance cell for conductance measurements performed using the pyrolytic boron nitride capillary.

B. Apparatus

1. Dry Box and Vacuum Line

Salts used in the experiments were stored, handled, and weighed inside a nitrogen filled dry box, due to their hygroscopic nature. A dry box (Vacuum Atmospheres Model

HE-43-2 DRI-LAB) employed a Model HE-63-P Pedatrol pressure controller, a Model HE-493 dry train containing molecular sieves to maintain a typical moisture level of < 2 ppm within the dry box, and a Panametrics model 70 Hygrometer, to monitor the moisture level within the dry box. All of the weighings were performed inside the dry box using a Sartorius electronic balance with a precision of 0.1 mg. Pre-purified nitrogen (Matheson gas, 99.998%) was used as a filler gas for the dry box.

For the storage of the purified salts outside the dry box, the salts were sealed under vacuum in Pyrex tubes. Fritted tubes (Ace Glass) were used to connect the Pyrex tubes to a vacuum manifold, which employed greaseless fittings and Teflon stopcocks (Ace Glass), via short segments of Tygon tubing. A Welch model 1516 three station thermocouple gauge and a Welch thermocouple probe were used to monitor the vacuum within the vacuum manifold; the pressure was usually less than 10 mTorr. A dry ice/acetone cold trap separated the vacuum manifold from a Welch Duo-Seal model 1402R vacuum pump. The cold trap was cleaned at least once every two weeks, or after warming to room temperature.

2. Furnace Assembly

The furnaces used were transparent gold furnaces (Trans Temp Co.). The gold furnaces (5.5 cm I.D. x 11 cm O.D. x 80

cm long) consisted of an inner quartz tube, a center quartz tube, an outer Pyrex tube possessing a thin gold layer for insulation, a 27 wound 45 cm long heating coil, and two ceramic bases. The heating coil was positioned between the inner and center quartz tubes. The quartz and Pyrex tubes were held in place using the two ceramic bases, with one base positioned at the top of the tubes and the other base positioned at the bottom of the tubes. The construction of the furnaces offered several advantages beside transparency. The versatility of the furnaces allowed them to be used in the vertical or horizontal position. A fast response time allowed for rapid heating and cooling. The heating element was easily interchangeable (usually less than 15 minutes), and provided an excellent temperature profile through 80% of its length. The gold furnaces were powered using a Lindberg Type 58114-P and a Lindberg Type 58114 controller. The variation in temperature of the furnace was typically within ± 1°C at 500°C and ± 2°C at 1000°C.

3. Cell Assembly

The basic cell design used for both the electrical conductance measurements and the emf measurements was of a "dip" type design, which is shown in Figure 5. Glassy carbon crucibles (Sigri, 4 cm O.D. x 3.5 cm I.D. x 5.6 cm long) and MgO crucibles (Custom Technical Ceramics, 4.3 cm O.D. x 3.8 cm I.D. x 5.5 cm long) were employed to contain

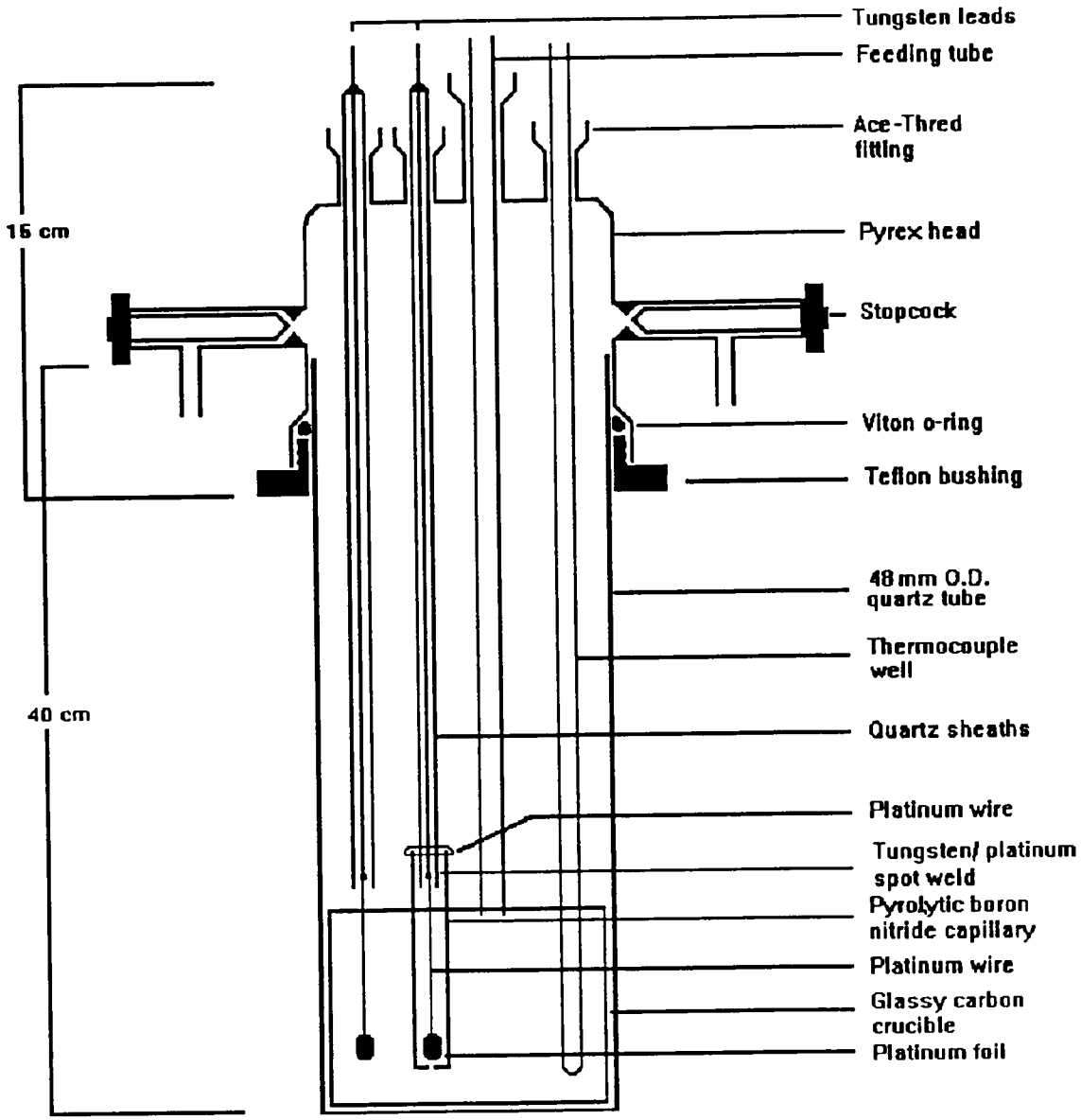


Figure 5. Conductance cell assembly.

the melts. Viton o-rings and Teflon bushings (Ace Glass, Inc.) were used to create vacuum tight seals between the Pyrex head and the quartz outer casing (48 mm O.D.), the electrode sheathing material (7 mm O.D.), and the thermocouple sheathing material (7 mm O.D.). The Pyrex head was constructed by sealing two # 15 Ace-Thred fittings, two # 7 Ace-Thred fittings, and two 0-4 stopcocks (Ace Glass, Inc.) to a # 50 mm Ace-Thred fitting. A feeding tube (Figure 6) was connected to the Pyrex head via a # 15 Ace-Thred fitting, and was used to make additions of the salts to the cell while at operating temperatures (800°C - 1000°C). A transfer apparatus (Figure 7), attached to the top of the feeding tube, was used to transport weighed amounts of salt from the dry box to the cell under inert atmosphere. The total length of the cell assembly was approximately 70 cm.

4. Conductance Measuring Equipment

Electrical conductance measurements were performed using the ac impedance method (90). An ac-impedance bridge built in-house at the University of Tennessee, high precision decade resistors and capacitors (General Radio), a HP model 209A oscillator, and a Tektronix type 549 storage oscilloscope, were used for the conductivity measurements. A home-made low frequency filter (f_c ~ 1 kHz), connected to the input of the detector, was employed to filter out line

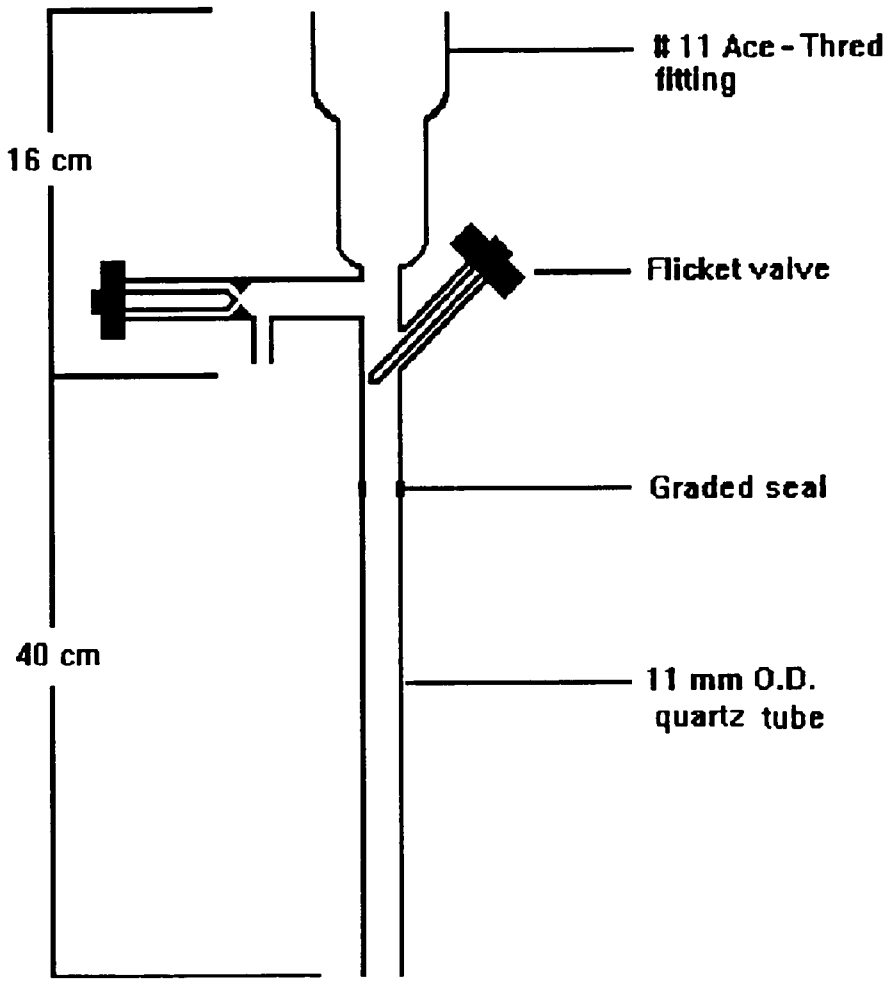


Figure 6. Feeding tube apparatus.

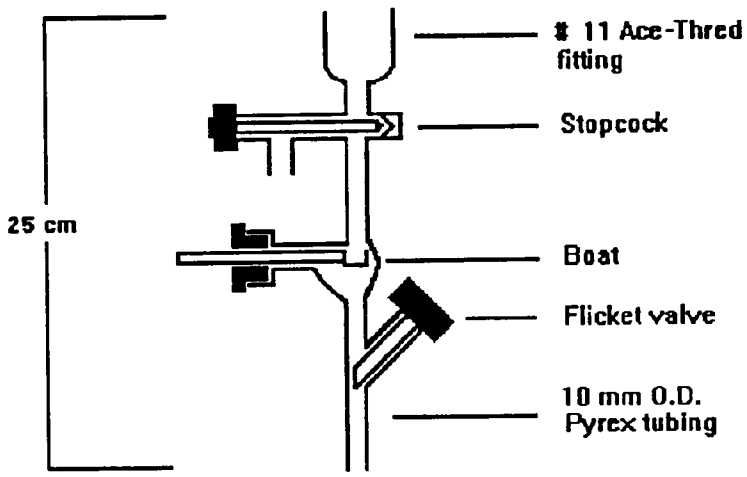


Figure 7. Apparatus used for the transfer of hygroscopic salts.

noise, and noise resulting from the furnace coils. The temperature of the furnaces was monitored using K-type (Chromel-Alumel) thermocouples (Omega). Either a home-made Pt/PtRh (13%) thermocouple, or a K-type thermocouple was used to monitor the temperature of the melt.

Platinum cylindrical electrodes were made by welding a platinum foil (ca. $1cm^2$) to a short segment of platinum wire. Electrical contact was made via a tungsten lead, which was either sealed in Pyrex tubing, as shown in Figure 8, or cemented (using Torr-Seal cement) in MgO sheathing materials, as shown in Figure 9. The design in Figure 8 was used to support the pyrolytic boron nitride capillary, since it could not be sealed in glass for support. The design in Figure 9 was used in conjunction with the MgO sheathing material. In both arrangements, the electrodes were connected to the conductance cell via Ace-Thred fittings.

5. EMF Measuring Equipment

Electromotive force measurements were made with a Keithley model 616 high impedance (> 10^{14} ohms) digital electrometer, which was calibrated against a Kintel standard cell (1.0193 ± 0.0005 V), and was in good agreement. Silver electrodes were constructed by spot welding an approximately 20 cm length of silver wire to a tungsten wire lead via a tiny piece of platinum foil. The upper length of the tungsten wire lead was sealed in Pyrex tubing, and fitted

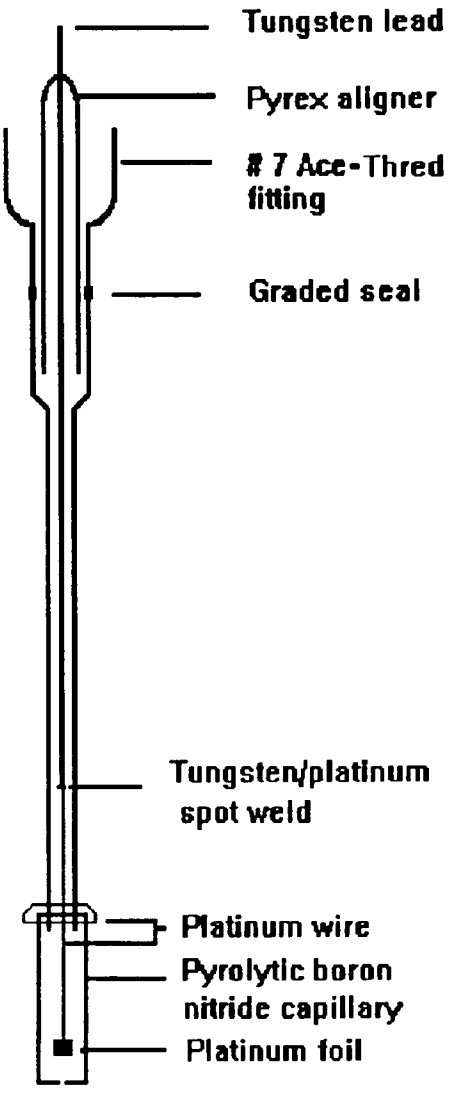


Figure 8. Electrode assembly used to support the pyrolytic boron nitride capillary.

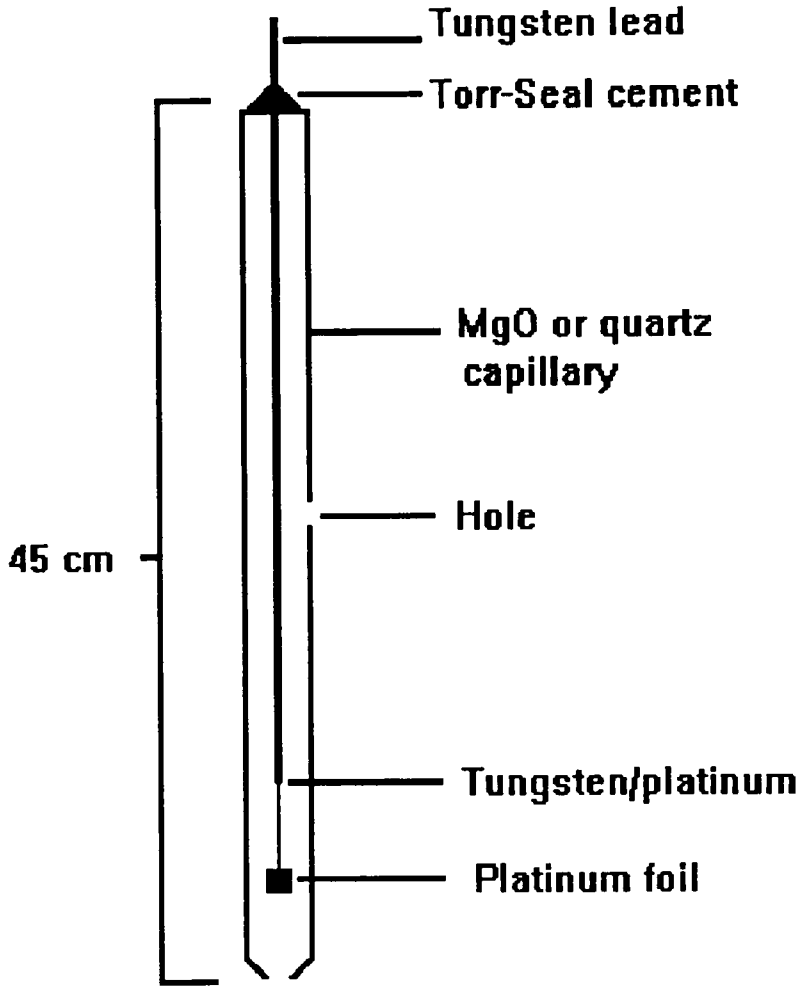


Figure 9. Electrode sealed in MgO or quartz tubing.

into the half-cell as shown in Figure 10. This design allowed for the elevation of the silver wire, and for easy removal of the silver wire for cleaning. Two types of reference half-cell membranes were used in the emf measurements, asbestos diaphragms and Vycor tubes. Reference half-cells employing asbestos plugs (Figure 10) were made according to the procedure followed by Flengas and Ingraham (74), and were used successfully in several KCl-NaCl (1:1 molar) molten salt systems. A segment of 6 mm O.D. quartz tubing was sealed at one end. Basically, a constriction of ca. 2 mm I.D. and ca. 3 mm above the closed end was made. A tightly rolled strand of asbestos fiber was placed in the quartz tube above the constriction and fired to a white ash under vacuum, in order to burn off any organic matter. At this point, caution was taken to prevent the asbestos from melting and sticking to the wall of the quartz tube. The asbestos fiber was then allowed to fall between the constriction, and the quartz tubing sealed at the construction by heating and squeezing with a pair of tweezers. The tube was then polished with an emery wheel, resulting in an asbestos capillary with an asbestos length of ca. 2 mm. Vycor reference half-cells (Figure 11) were made by torch sealing an approximately 6 cm length of Vycor to a quartz sheath, and blowing the end of the Vycor to a mechanically stable thin membrane (< 0.25 mm). The upper section of both reference half-cells was constructed from

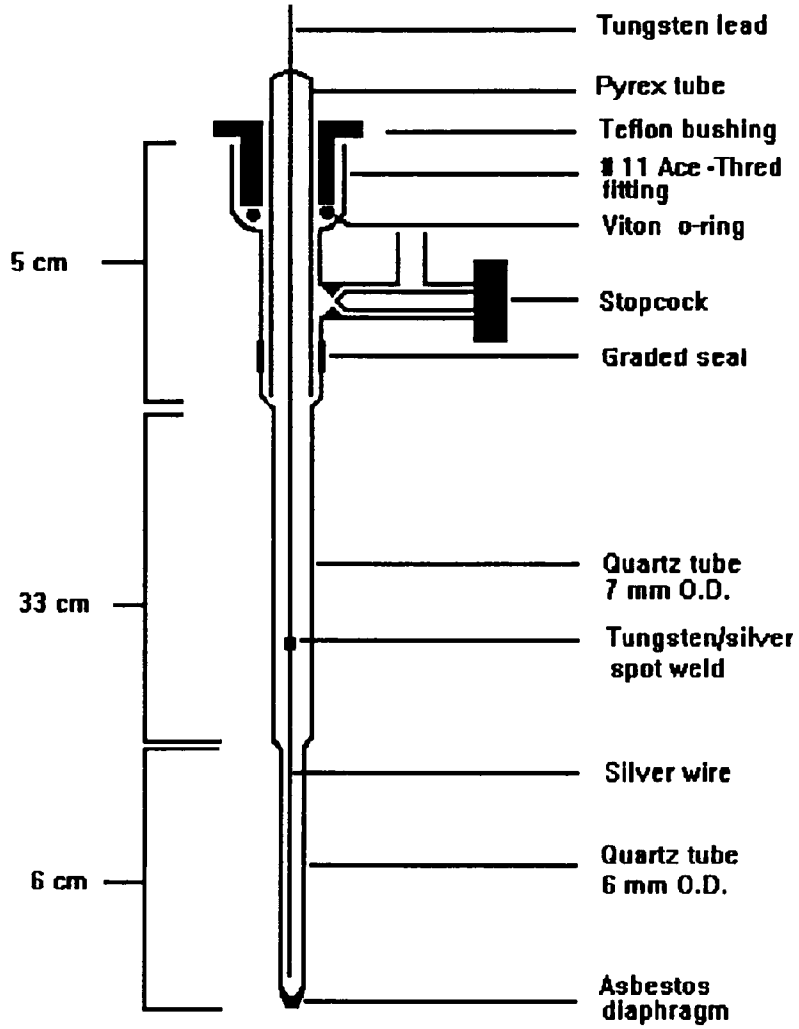


Figure 10. Reference half-cell with an asbestos diaphragm.

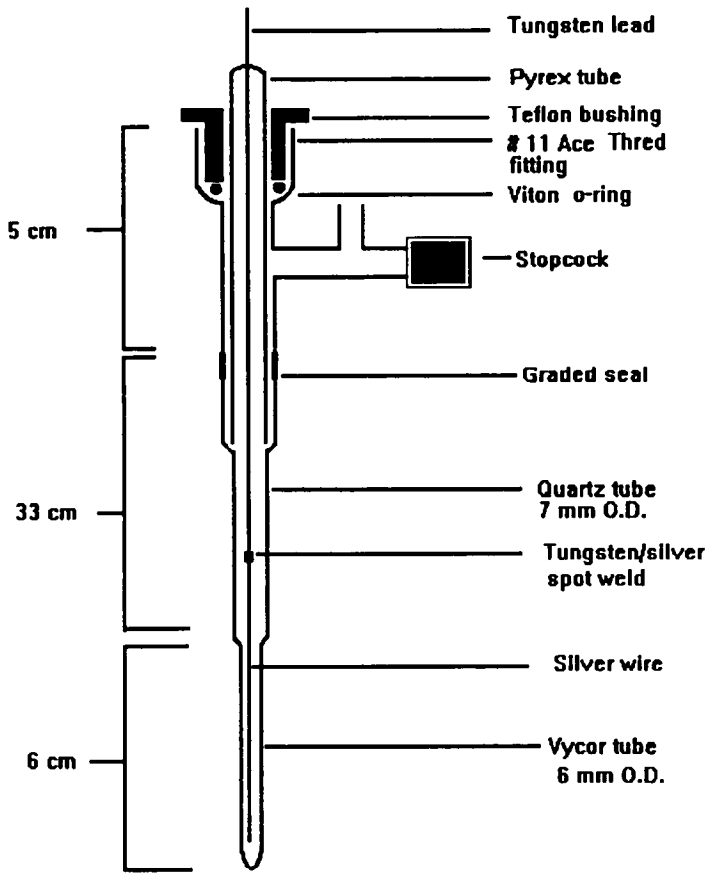


Figure 11. Reference half-cell with a Vycor membrane.

Pyrex glass, which allowed for the reference half-cell to be placed under vacuum or under a flow of nitrogen by connecting a stopcock.

C. Procedure

1. Cleaning Procedures

The Pyrex and quartz cell parts were cleaned by soaking in 6 M HCl, followed by a thorough rinsing with distilled water. The glassy carbon crucible was cleaned by soaking in a triple acid mixture of $HCl:HNO_3:HF:H_2O$ (1:1:0.25:10 by volume, respectively), followed by boiling in distilled water at least three times, along with sonication for several minutes. The tungsten wires used in the preparation of the electrodes were cleaned by first soaking in the triple acid mixture, followed by a soaking in a 45% NaOH - 55% $NaNO_2$ solution, and a thorough rinsing with distilled water. The platinum wire electrodes were cleaned by dipping in a warm solution of concentrated $HCl:HNO_3$ (1:1 by volume), followed by a thorough rinsing in distilled water. All of the Teflon bushings and o-rings were cleaned by boiling in 6 M HCl.

2. Conductance Measurements

In earlier experiments, the conductivity cell was calibrated using a 1 demal KCl solution at 0°C (35) and a

1 N NaCl solution at 18°C; agreement was usually within 1%. For the experiments employing the pyrolytic boron nitride capillary, molten KCl and molten NaCl were used for the calibration of the cell. The cell constant, determined using molten KCl at 820°C and molten NaCl at 820°C for a set of electrodes, typically ranged from 47.94 cm^{-1} to 47.40 cm^{-1}, respectively. Slight deviations from this range of cell constants were observed for different sets of electrodes, since electrodes were dismantled for cleaning. The conductivity cell was checked for leaks by placing it under vacuum (ca. 10 mTorr), and monitoring the vacuum within the vacuum manifold with the cell opened to the vacuum manifold and the vacuum manifold shut off from the cold trap. If no leaks were detected, the cell was dried under vacuum (ca. 10 mTorr) at 800°C for at least 48 hours before being transferred to the dry box, where a known amount of purified $CaCl_2$ was added to the cell and the transfer vessel. The cell was then positioned within the furnace with the Pyrex head protruding from the top of the furnace and cooled by a stream of compressed air. To avoid the buildup of pressure within the cell at the elevated temperatures, the cell was placed under a low flow of dry nitrogen until the operating temperature was reached, at which time the cell was shut off from the flow of nitrogen. The transfer apparatus was then connected to the feeding tube, and the portion between the two devices flushed with

dry nitrogen for at least one hour. In all of the experiments, the conductivity of purified $CaCl_2$ was measured before making an addition of CaO. The frequency dispersion of the melt was determined before each experiment by extrapolating measured resistances, acquired at several frequencies, to infinite frequency. For each experiment, the frequency at which the resistance became constant was used for all of the measurements in that experiment. Electrical conductivity values were determined, in the temperature range 790°C - 990°C, by balancing the impedance of the cell with a variable resistor and capacitor, and substituting these values into equations (2) and (4), pp. 5 and 9, respectively. After measuring the conductivity of purified $CaCl_2$ at several increasing and decreasing temperatures, an addition of CaO was made. After the addition of CaO, the transfer apparatus was transferred to the dry box for a subsequent weighing of CaO. The use of the transfer vessel eliminated the necessity to freeze the melt and transport the conductance cell to the dry box for an addition of the CaO. The cell was allowed to remain at the maximum operating temperature (usually 990°C) for approximately 1 hour to assure complete dissolution of the CaO. The resistance was then measured following the procedure used for purified $CaCl_2$.

3. Potentiometry

The emf cell was checked for leaks following the procedure described in Section 2, p. 42. If no leaks were detected, the cell and its contents were dried for at least 48 hours under vacuum, before being transferred to a dry box, where weighed amounts of salts were added to their respective compartment. The initial AgCl concentration in the sample compartment was usually 0.01 mole fraction; subsequent additions were made with the cell at operating temperatures. A pre-melted $CaCl_2$-AgCl (0.05 mole fraction of AgCl) melt served as the reference melt. The "pre-melted" melt was used for many experiments; two "pre-melted" $CaCl_2$-AgCl (0.05 mole fraction of AgCl) melts were used for all of the emf experiments. The pre-melted melts were stored inside a dark container wrapped with aluminum foil to minimize photodecomposition of AgCl. To avoid the buildup of pressure at the elevated temperatures, both compartments were placed under a low flow of dry nitrogen until the operating temperature was reached, at which time the compartments were shut off from the flow of nitrogen. A temperature ramp was used to increase and decrease the temperature of the cell at a typical rate of ca. 10°C/minute. After lowering the electrodes into the melt, the potential was monitored for at least 1 hour after becoming stable, during which time the next sample of salt was being prepared. Only one hour was allowed for the

potential to become stable within 0.3 mV due to the corrosiveness of the melt, and as a result, an experiment lasted only ca. 50 hours. The transfer apparatus was then connected to the feeding tube, and the portion between the two devices flushed with dry nitrogen for at least one hour. After a stable potential was achieved, an addition of salt was made, and the transfer apparatus transferred into the dry box for another weighing of salt. At selected AgCl compositions, potentials were recorded for both increasing and decreasing temperatures in the range 800°C to 950°C.

CHAPTER 3

RESULTS AND DISCUSSION: CONDUCTANCE MEASUREMENTS OF $CaCl_2$-CaO MELTS

A. INTRODUCTION

The specific conductivity, κ, of molten $CaCl_2$ was determined by measuring the resistance between bright platinum cylindrical electrodes in the temperature range 790°C to 990°C, using a conventional ac technique. For each new set of electrode sheathing materials, the variation of the resistance with frequency (frequency dispersion) was determined by extrapolation of the measured resistance to infinite frequency, since the frequency dispersion was determined to be dependent upon the cell constant (44). Sheathing materials were employed to obtain a larger cell constant, since cells with no sheathing materials resulted in measured resistances on the order of 1 to 5 ohms, which were too low for accurate measurements. At the beginning of this study, it was learned that at Los Alamos National Laboratory MgO crucibles were used to contain $CaCl_2$-CaO melts (20). Magnesia tubes, magnesia capillaries, and a pyrolytic boron nitride capillary (0.76 mm I.D.) were used as sheathing materials for conductance measurements of $CaCl_2$-CaO melts.

B. Conductivity Measurements Using MgO Tubes

Preliminary results of the conductivity of $CaCl_2$-CaO melts have been reported by Flowers and Mamantov (91), who employed 3 mm I.D. MgO tubes to sheath bright platinum cylindrical electrodes. Cell constants ranged from 60 cm^{-1} (for virgin tubes) to 30 cm^{-1} (for used tubes). Extrapolations of the measured resistance of molten $CaCl_2$ versus $\omega^{-1/2}$ and versus f (kHz) to infinite frequency are shown in Figures 12 and 13, respectively; the data are given in Table 1. Since the extrapolation in Figure 13 is more readily attained compared to Figure 12 and appears to give frequency-independent resistances, it is shown in the remaining sections. From Figure 13, a constant resistance was achieved at ca. 20 kHz; thus, in all of the experiments employing MgO sheaths, an ac frequency of 30 kHz was used to assure minimal polarization effects. The resistance values in Table 1 give an indication of the precision of the measured resistances for the experiments employing MgO tubes.

Figure 14 shows conductance isotherms obtained from three separate series of experiments which were consistent in exhibiting two minima occurring at ca. 6 mole percent CaO and 11 mole percent CaO in the temperature range 800°C to 950°C obtained by Flowers (91). Each experiment began by

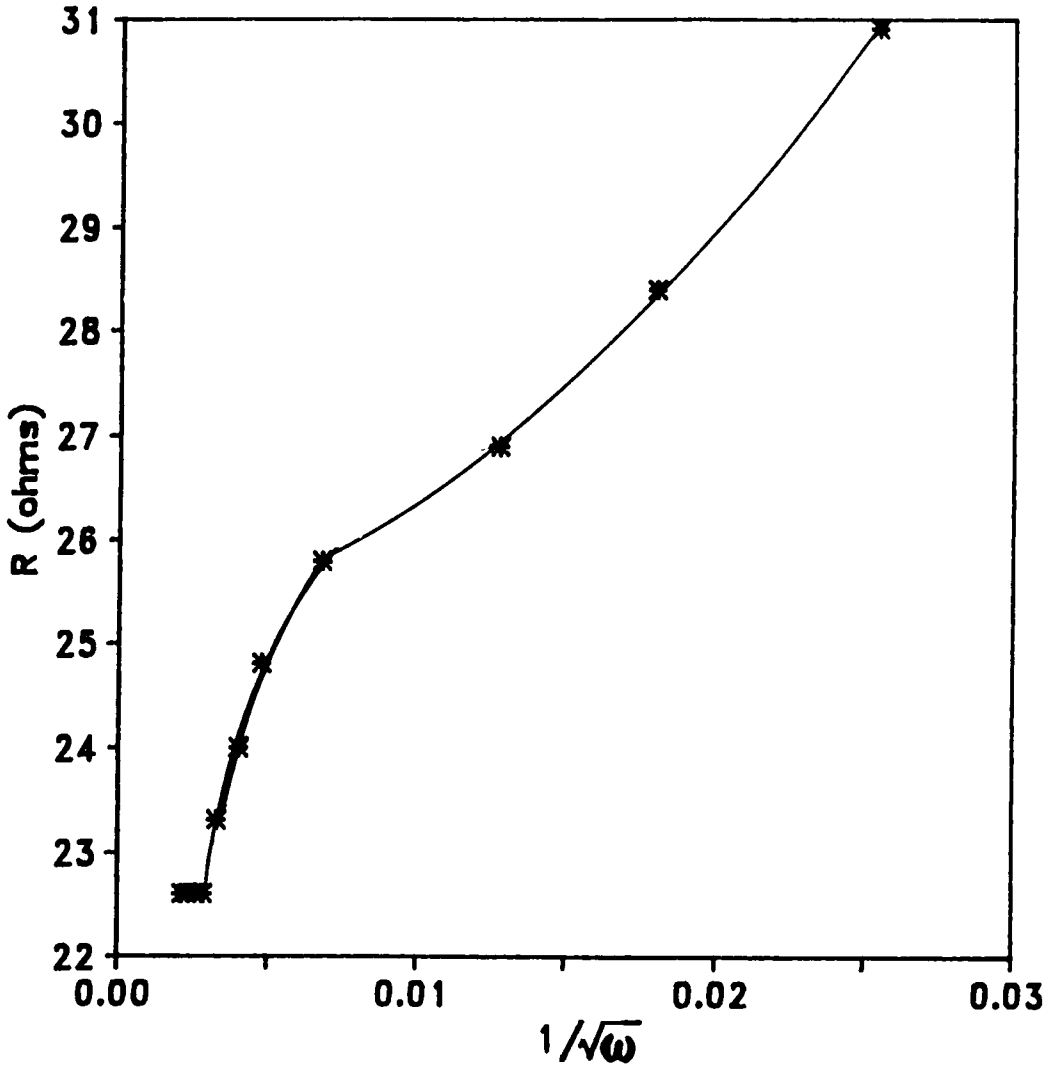


Figure 12. Frequency dispersion of the resistance of molten $CaCl_2$ at 800°C using magnesia sheathing tubes (data taken from Ref. 91).

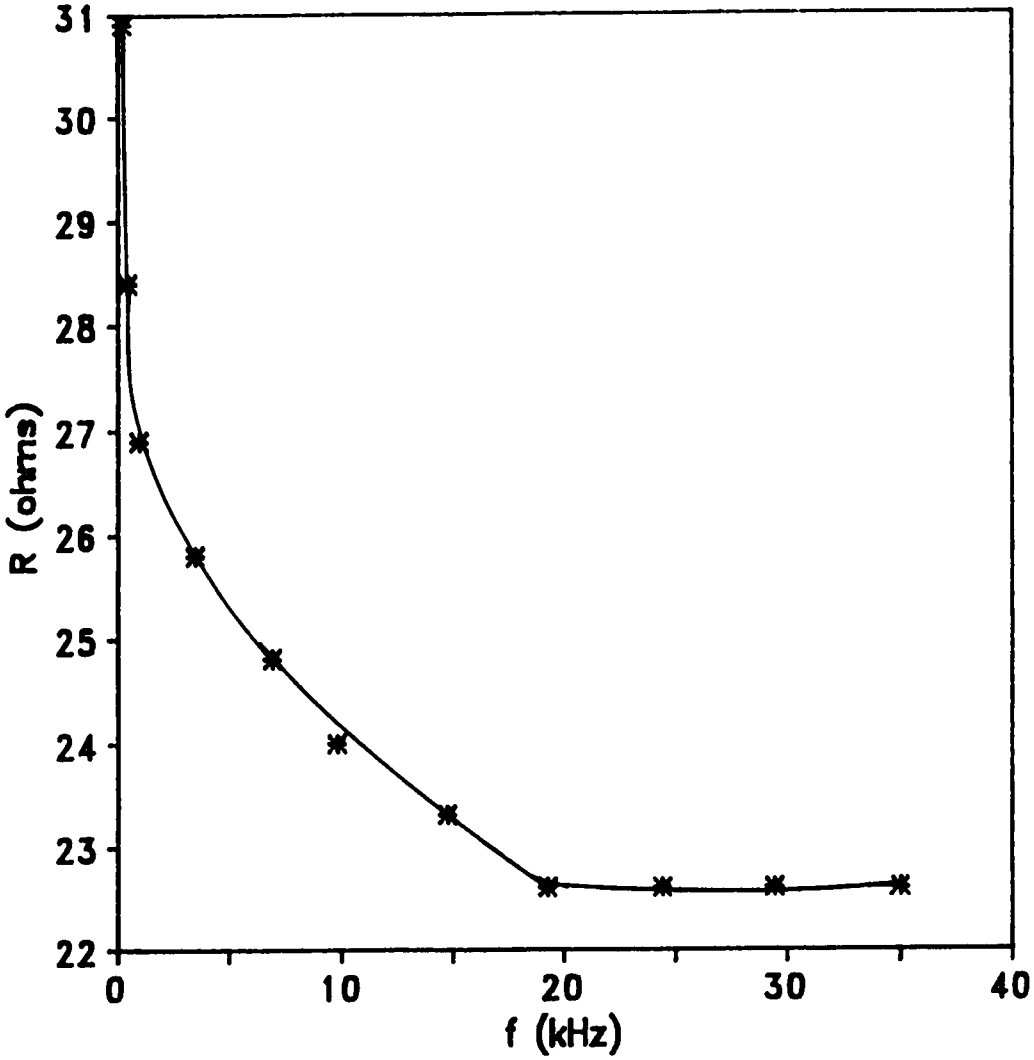


Figure 13. Plot of measured resistance versus frequency for molten $CaCl_2$ at 800°C using magnesia sheathing tubes (data taken from Ref. 91).

Table 1

Frequency dispersion of the resistance of molten $CaCl_2$ at 800°C using MgO tubes (data from Ref. 91)

Frequency (kHz)	$\omega^{-1/2}$	R (ohms)
0.247	0.0254	30.9
0.494	0.0179	28.4
0.980	0.0127	26.9
3.448	0.0067	25.8
6.944	0.0048	24.8
9.804	0.0040	24.0
14.71	0.0033	23.3
19.23	0.0029	22.6
24.39	0.0025	22.6
29.41	0.0023	22.6
35.00	0.0021	22.6

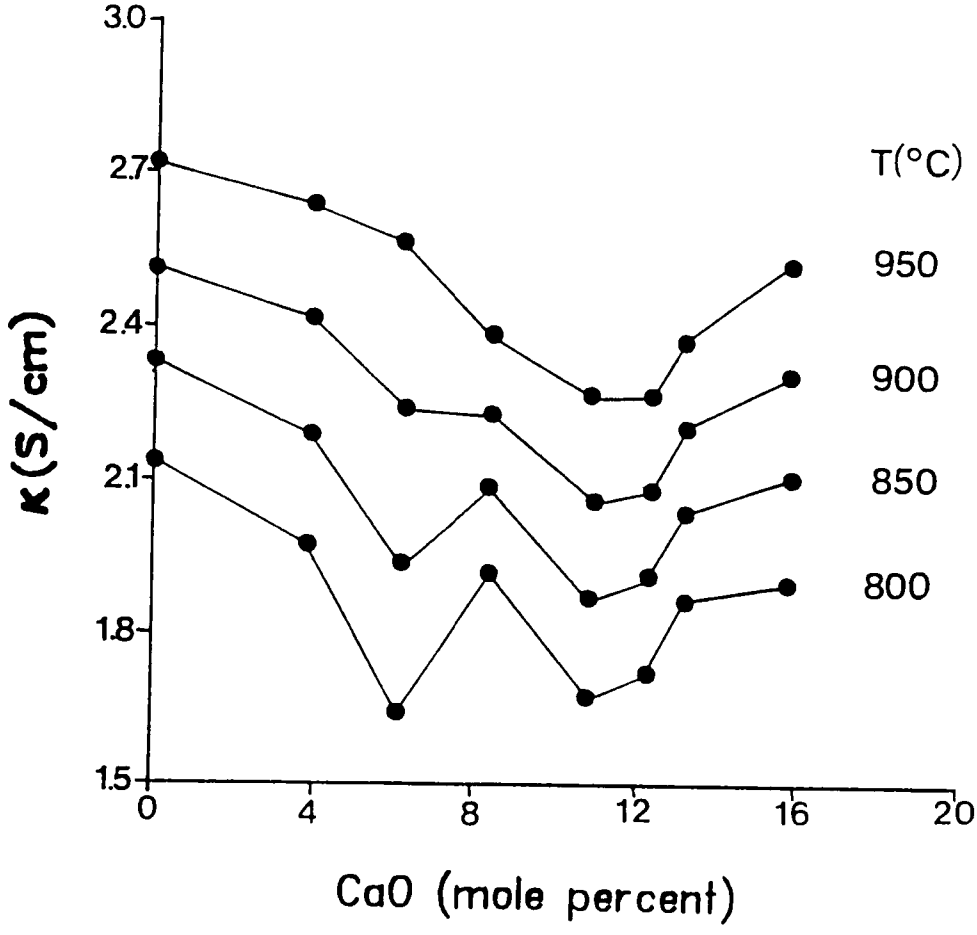


Figure 14. Conductance isotherms for molten $CaCl_2$-CaO using magnesia sheathing tubes (data taken from Ref. 91).

measuring the conductance of pure $CaCl_2$ followed by five CaO additions. It should be noted here that an experiment involved the measurement of the conductance at several increasing and decreasing temperatures beginning with pure $CaCl_2$ through several additions of CaO. The minimum at 6 mole percent CaO corresponded to the eutectic composition of the $CaCl_2$-CaO system (Figure 1, p. 4), however, the temperatures at which the measurements were performed were above the melting point of the eutectic (ca. 770°C). Flowers (91) did not attempt to explain the observations; however, he noted that there was no definite dependence of the activation energy for conductance with the increase in the CaO concentration (Figure 15). Flowers also observed a decrease in the cell constant using the same MgO tubes with successive experiments; no explanation was provided for this observation.

Additional conductivity studies of $CaCl_2$-CaO melts by this author were not in agreement with the results of Flowers (91). Figures 16-18 represent conductance isotherms obtained following the same experimental procedure used by Flowers (91). The data are summarized in Tables 2-4, respectively. It may be seen that the conductance isotherms in Figures 14 (p. 52) and 16-18 are not reproducible. The conductivity of molten $CaCl_2$ from Figures 16-18 (Figure 19) was reproducible within 7% to 12% at 790° and 990°C, respectively, but deviated between 10% to 24% from the

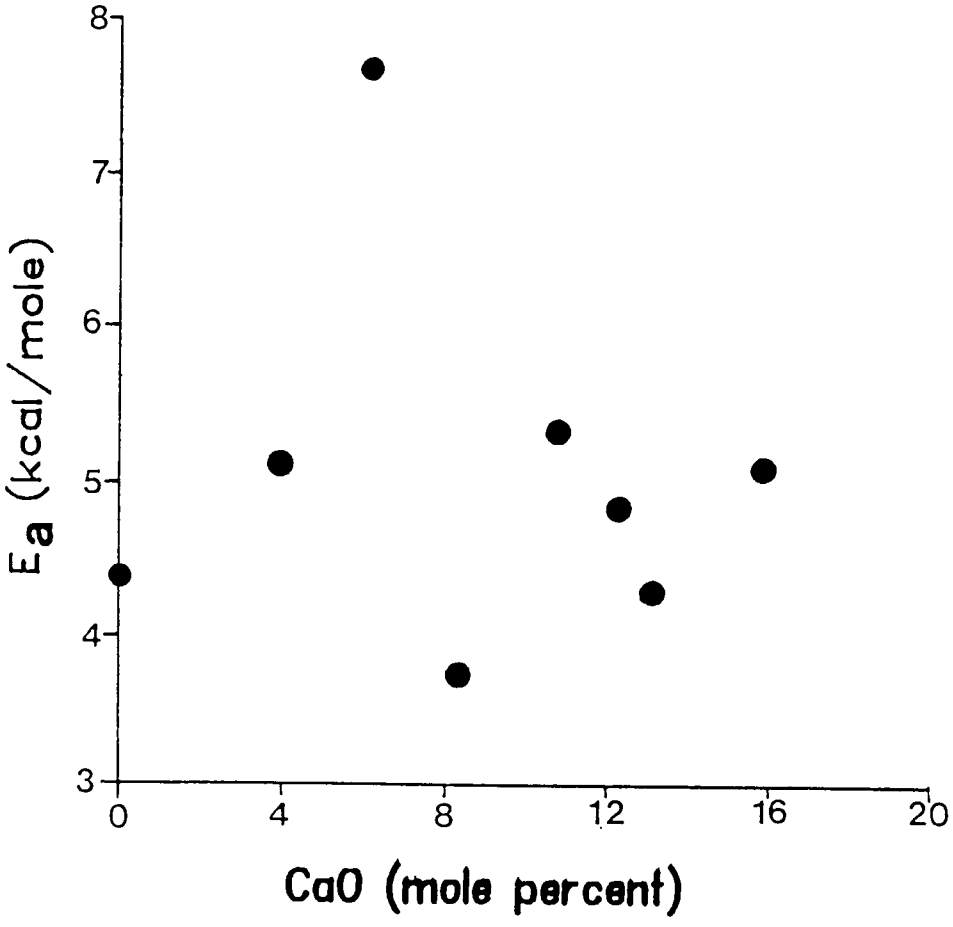


Figure 15. Activation energy versus CaO concentration (data taken from Ref. 91).

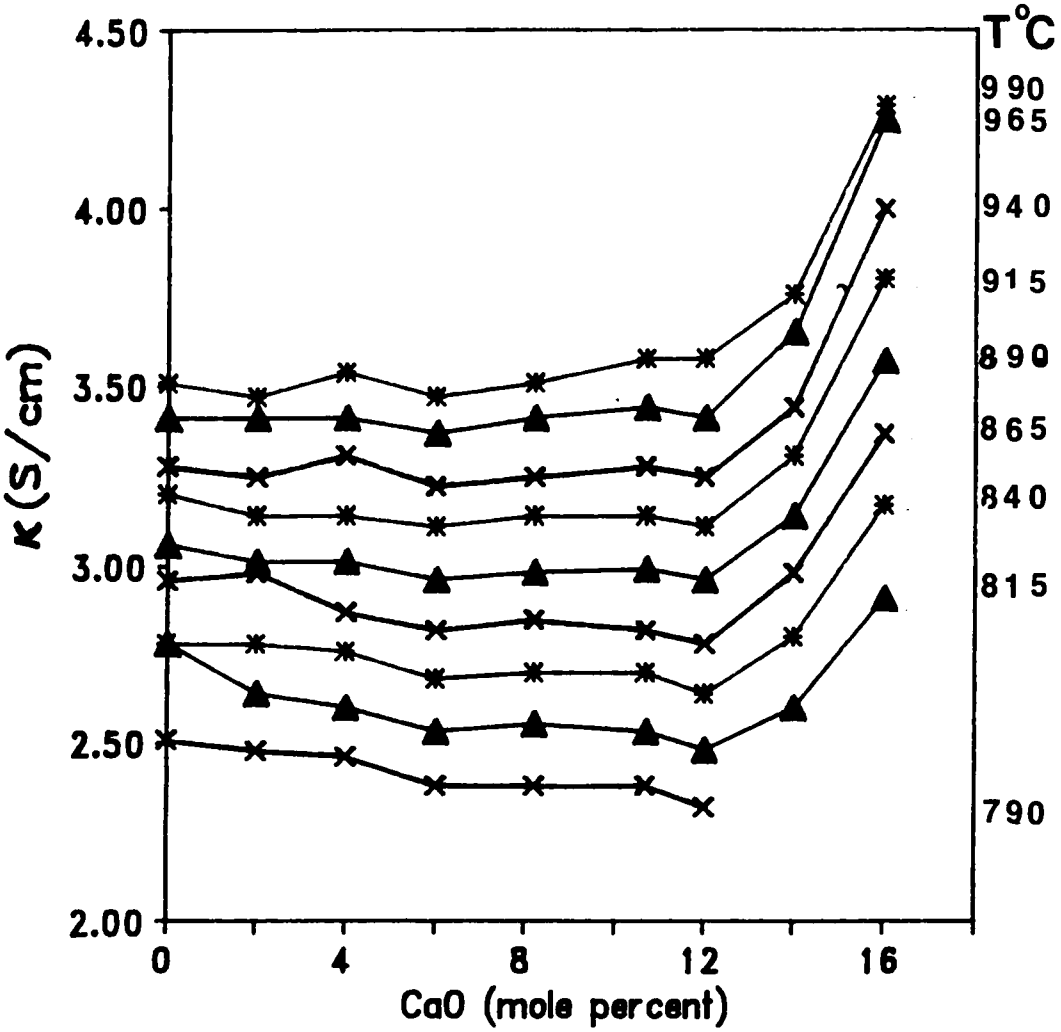


Figure 16. Conductance isotherms for the $CaCl_2$-CaO system using MgO sheathing tubes: Experiment #1.

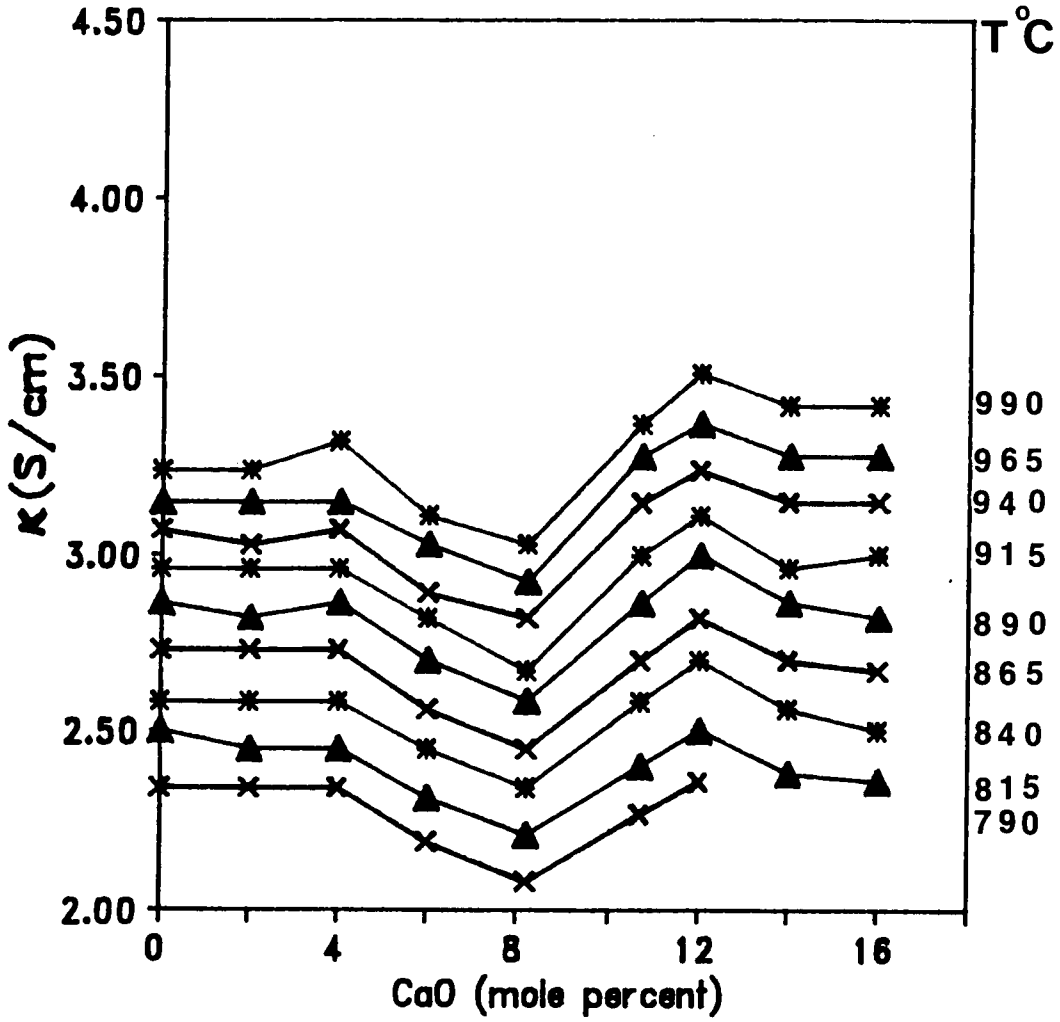


Figure 17. Conductance isotherms for the $CaCl_2$-CaO system using MgO sheathing tubes: Experiment #2.

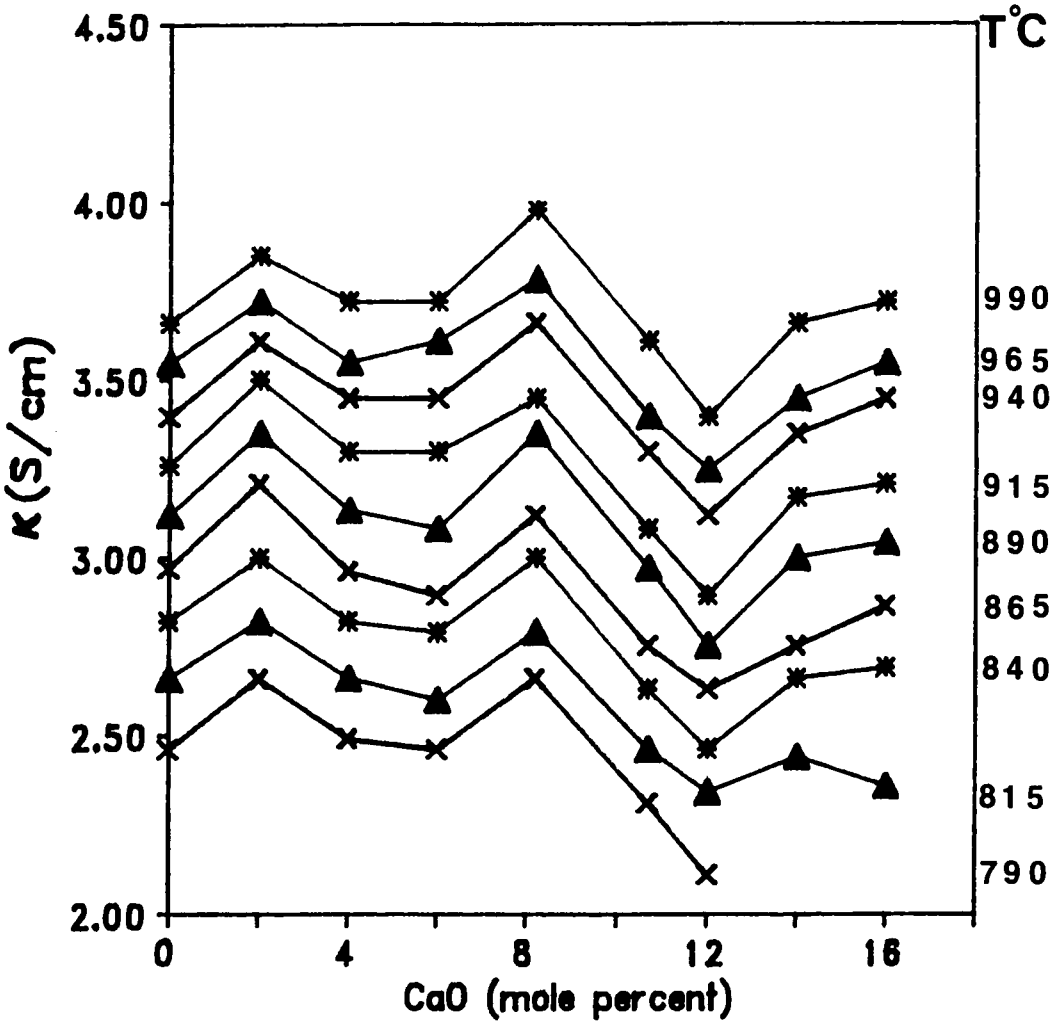


Figure 18. Conductance isotherms for the $CaCl_2$-CaO system using MgO sheathing tubes: Experiment #3.

Table 2

Specific Conductivity Data for a $CaCl_2$-CaO melt at 30 kHz: Experiment #1

Temperature (°C)	Specific Conductivity (S/cm)								
	(CaO) mole percent								
	0	2	4	6	8.5	10.7	12	14	16
790	2.51	2.48	2.46	2.38	2.38	2.38	2.32	----	----
815	2.78	2.64	2.60	2.53	2.55	2.53	2.48	2.60	2.91
840	2.78	2.78	2.76	2.68	2.70	2.70	2.64	2.80	3.17
865	2.96	2.89	2.87	2.82	2.85	2.82	2.78	2.98	3.37
890	3.06	3.01	3.01	2.96	2.98	2.99	2.96	3.14	3.57
915	3.20	3.14	3.14	3.11	3.14	3.14	3.11	3.31	3.80
940	3.28	3.25	3.31	3.22	3.25	3.28	3.25	3.44	4.00
965	3.41	3.41	3.41	3.37	3.41	3.44	3.41	3.65	4.25
990	3.51	3.47	3.54	3.47	3.51	3.58	3.58	3.76	4.29

Table 3

Specific Conductivity Data for a $CaCl_2$-CaO melt at 30 kHz: Experiment #2

Temperature (°C)	Specific Conductivity (S/cm)								
	(CaO) mole percent								
	0	2	4	6	8.2	10.7	12	14	16
790	2.34	2.34	2.34	2.19	2.08	2.27	2.36	----	----
815	2.50	2.45	2.45	2.31	2.21	2.40	2.50	2.38	2.36
840	2.58	2.58	2.58	2.45	2.34	2.58	2.70	2.56	2.50
865	2.73	2.73	2.73	2.56	2.45	2.70	2.82	2.70	2.67
890	2.86	2.82	2.86	2.70	2.58	2.86	3.00	2.86	2.82
915	2.96	2.96	2.96	2.82	2.67	3.00	3.11	2.96	3.00
940	3.07	3.03	3.07	2.89	2.82	3.15	3.24	3.15	3.15
965	3.15	3.15	3.15	3.03	2.92	3.28	3.37	3.28	3.28
990	3.24	3.24	3.32	3.11	3.03	3.37	3.51	3.42	3.42

Table 4

Specific Conductivity Data for a $CaCl_2$-CaO melt at 30 kHz: Experiment #3

Temperature (°C)	Specific Conductivity (S/cm)								
	[CaO] mole percent								
	0	2	4	6	8.2	10.7	12	14	16
790	2.46	2.66	2.49	2.46	2.66	2.31	2.11	——	——
815	2.66	2.82	2.66	2.60	2.79	2.46	2.34	2.44	2.36
840	2.82	3.00	2.82	2.79	3.00	2.63	2.46	2.66	2.69
865	2.97	3.21	2.96	2.89	3.12	2.75	2.63	2.75	2.86
890	3.12	3.35	3.13	3.08	3.35	2.97	2.75	3.00	3.04
915	3.26	3.50	3.30	3.30	3.45	3.08	2.89	3.17	3.21
940	3.40	3.61	3.45	3.45	3.66	3.30	3.12	3.35	3.45
965	3.55	3.72	3.55	3.61	3.78	3.40	3.25	3.45	3.55
990	3.66	3.85	3.72	3.72	3.98	3.61	3.40	3.66	3.72

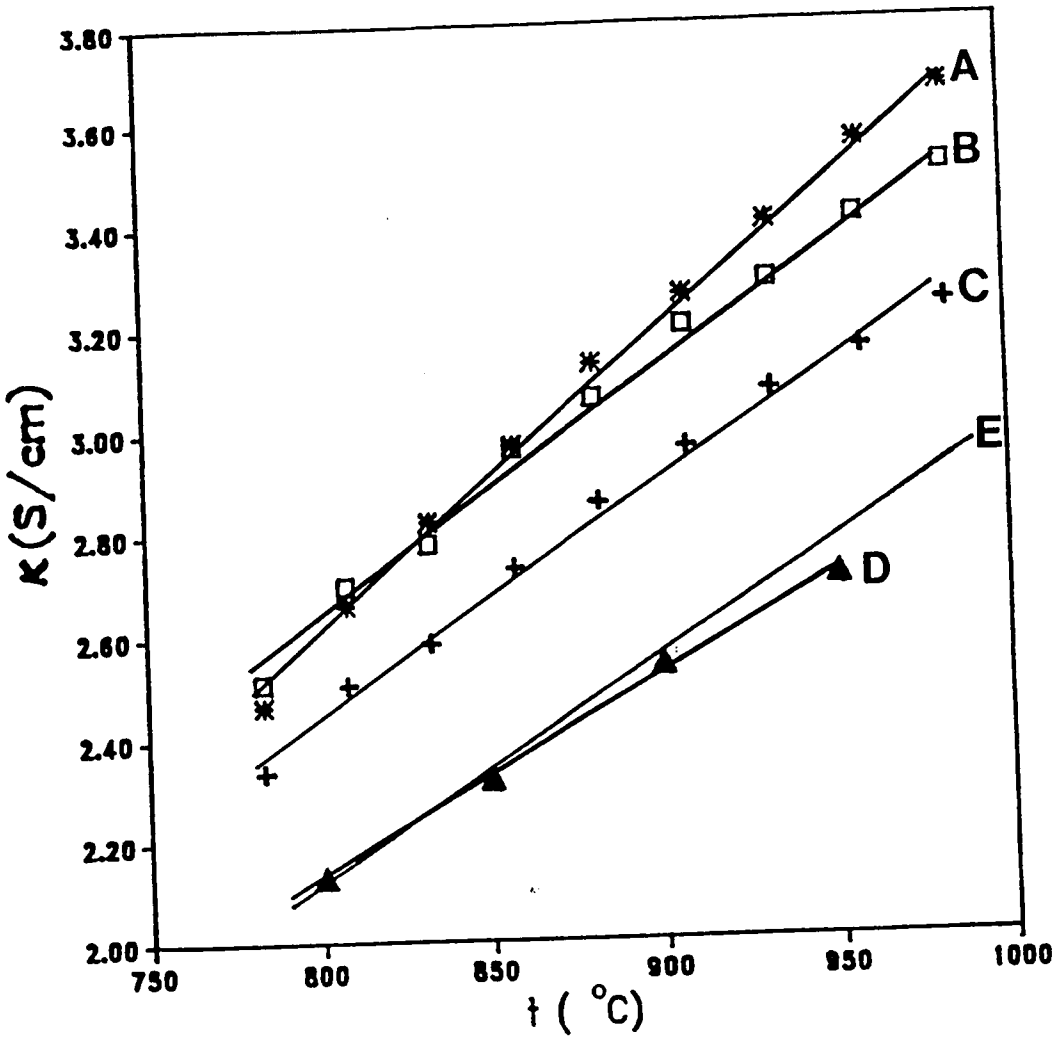


Figure 19. Specific conductivity of molten $CaCl_2$: (A) data from Figure 18; (B) data from Figure 16; (C) data from Figure 17; (D) data from Figure 14 (Ref. 91); (E) recommended data (ref. 48).

recommended data (48). The observed deviations in the conductance data may have resulted from various factors. For instances, the cell constant was observed to decrease after each experiment, as shown in Figure 20. This observation was presumably caused by the attack of the MgO tubes by the melt. Also, the measured resistance for molten $CaCl_2$ in Figures 16-18 (pp. 55-57) ranged from 14.4 ohms at 790°C to 10.3 ohms at 990°C, 10.8 ohms at 790°C to 7.9 ohms at 990°C, and 9.9 ohms at 790°C to 6.8 ohms at 990°C, respectively, with an accuracy of ± 0.1 ohm. Although the conductance isotherms in Figures 16-18 (pp. 55-57) showed no definite trends, plots of ln κ vs. 1/T (K) (Figure 21) were observed to be linear with correlation coefficients of 0.99, indicating that the Arrhenius equation (equation (3), p.7) was obeyed.

The activation energy for conduction, determined for the slope of equation (3) (p.7), was observed to increase with an increase in the CaO concentration, unlike the data by Flowers shown in Fig. 15, p. 54. Figure 22 shows the variation in the activation energy for the three experiments shown in Figures 16-18 (pp. 55-57); the data are summarized in Table 5. Figure 23 shows three sets of the conductivity data for molten $CaCl_2$ in the temperature range 790°C - 990°C, using the same MgO tubes and a cell constant of 21.15 cm^{-1}; the melt was frozen with the electrodes in place

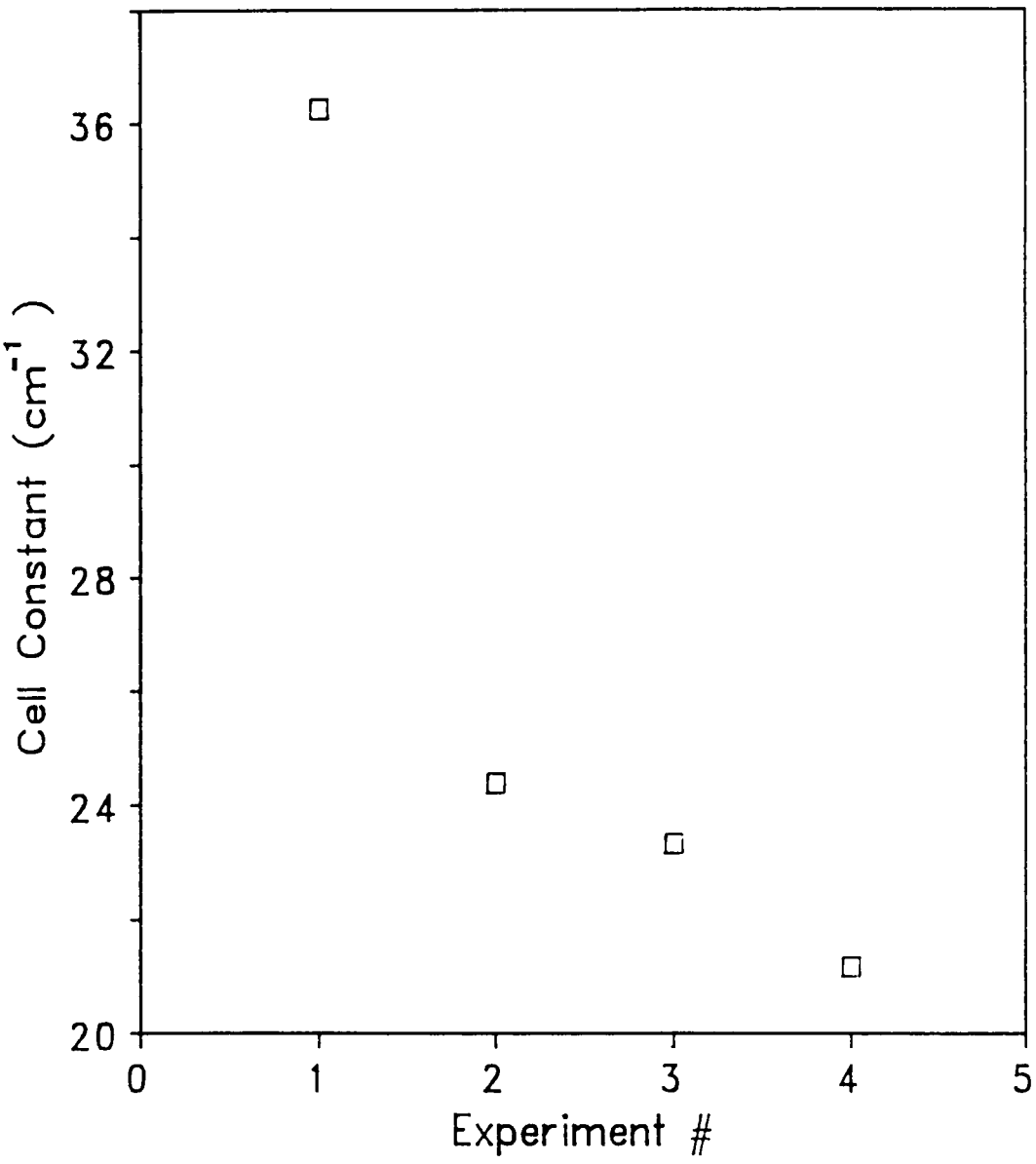


Figure 20. Variation of the cell constant using magnesia sheathing tubes.

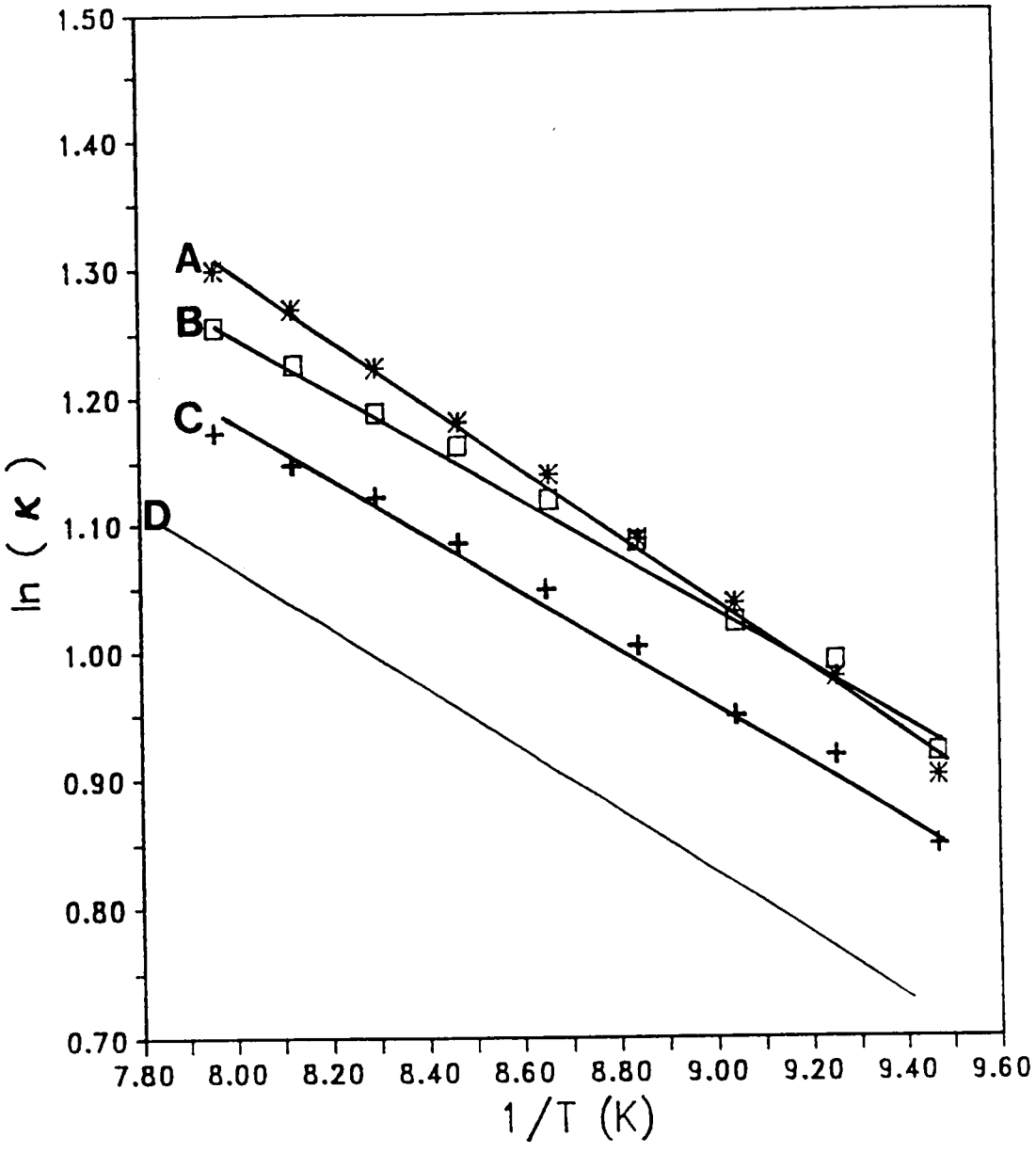


Figure 21. Arrhenius plots for the $CaCl_2$-CaO (0 - 14 mole percent CaO) system using magnesia sheathing tubes: (A) data from Figure 18; (B) data from Figure 16; (C) data from Figure 17; (D) recommended data (ref. 48).

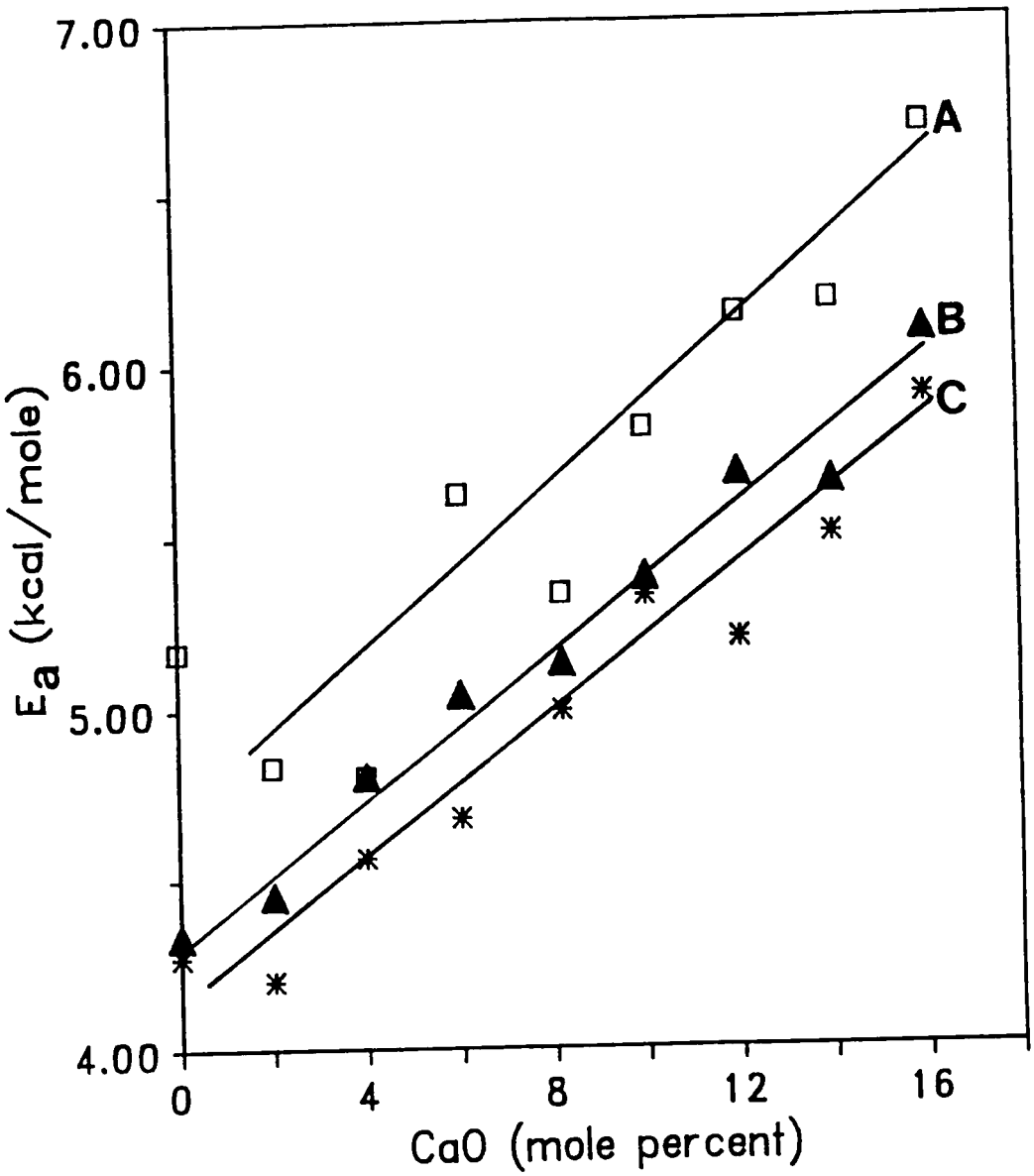


Figure 22. Activation energy for molten $CaCl_2$-CaO using magnesia sheathing tubes: (A) data from Figure 18; (B) data from Figure 16; (C) data from Figure 17.

Table 5

Activation energy (kcal/mole) for the $CaCl_2$-CaO system

CaO (mole fraction)	Plot		
	A*	B*	C*
0	5.17	4.33	4.27
2	4.84	4.44	4.21
4	4.81	4.80	4.09
6	5.62	5.04	4.96
8.2	5.34	5.11	5.00
10.7	5.82	5.33	5.32
12	6.14	5.69	5.20
14	6.18	5.64	5.50
16	6.70	6.09	5.91

*See Fig. 22.

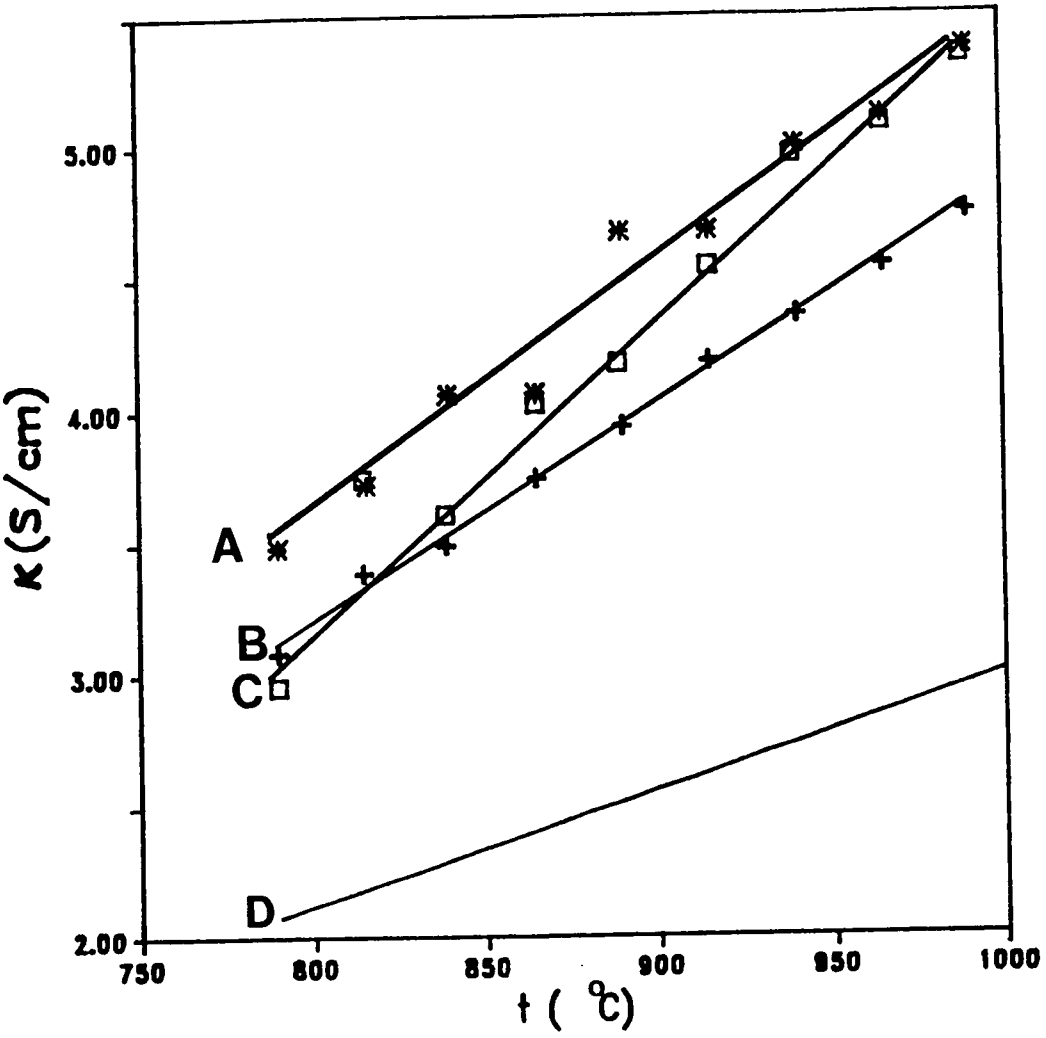


Figure 23. Specific conductivity data of molten $CaCl_2$: (A) data set #3; (B) data set #1; (C) data set #2; (D) recommended data (ref.48).

after each set. The measured resistances ranged from 7.6 ohms to 4.4 ohms at 790°C to 990°C, respectively. The data showed deviations of 42% to 67% from the recommended data (48) and showed deviations from 12% to 16% between the three sets of measurements. After the experiments, the MgO tubes were observed to possess tiny pits, suggesting an attack by the melt.

C. Conductivity Measurements Using MgO Capillaries

It was attempted to increase the resistance measured by constructing the electrodes using MgO capillaries (ca. 1 mm I.D. tips). An ac frequency of 30 kHz was also used for these measurements. Although a larger cell constant was obtained (108 cm^{-1}), which increased the measured resistances in the range of 33 - 45 ohms at 990°C to 790°C, respectively, the conductance of pure $CaCl_2$ (Figure 24, points labeled □), showed a 16% - 20% deviation from the recommended data (48). An additional experiment (Figure 24, points labeled *), using a cell constant of 80.8 cm^{-1}, resulted in measured resistances ranging from 21 ohms to 30 ohms, and showed a 30% to 36% deviation from the recommended data. A summary of the data in Figure 24 is shown in Table 6. After using the MgO capillaries in the CaO-containing melt, they possessed the same surface features as

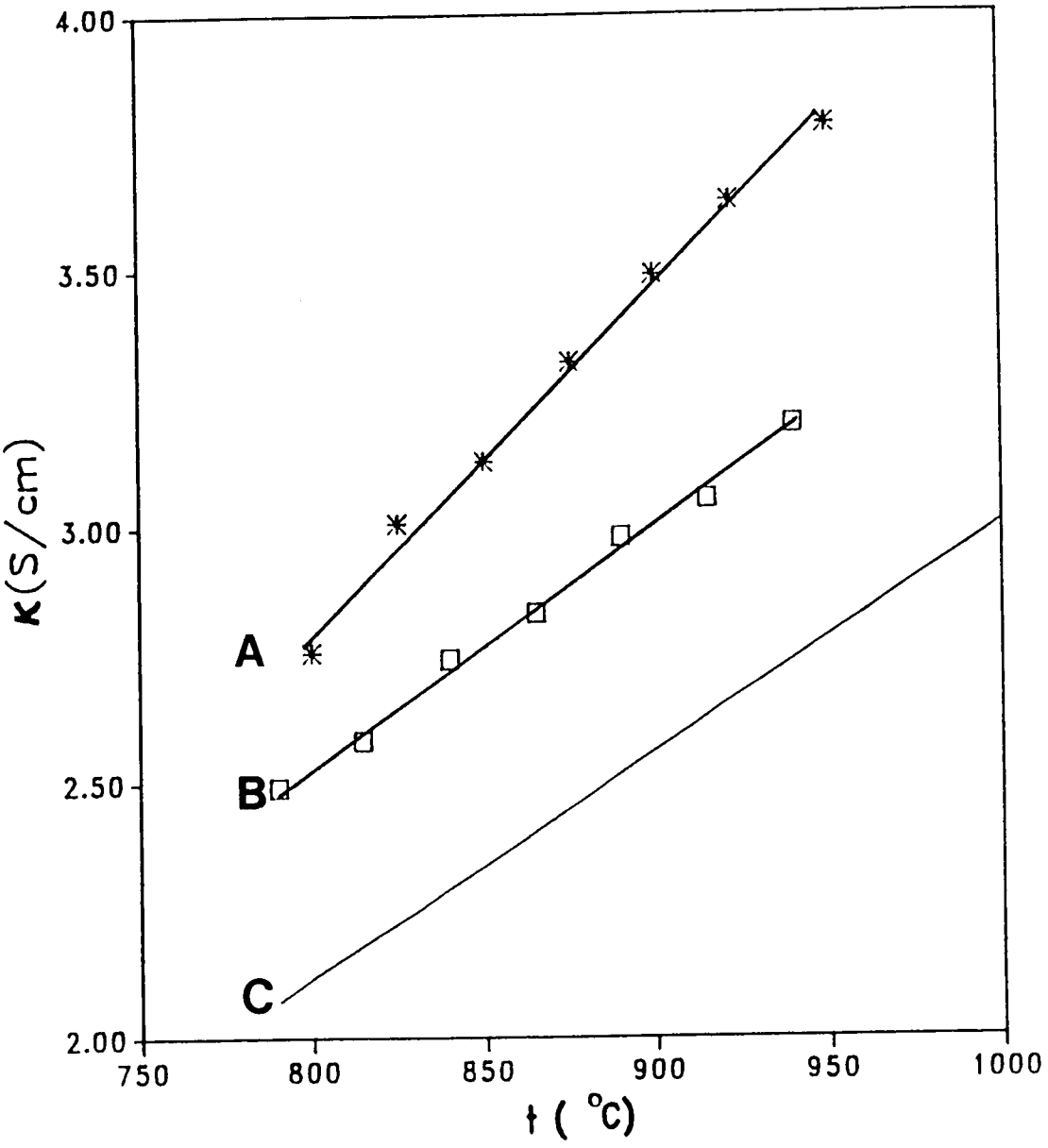


Figure 24. Specific conductivity data of molten $CaCl_2$ using magnesia capillaries: (A) and (B) two sets of measurements; (C) recommended data (ref. 48).

Table 6

Specific Conductivity Data for a $CaCl_2$ melt at 30 kHz using MgO capillaries

Temperature (°C)	Specific Conductivity (S/cm)		
	A*	B*	C*
790	2.49		2.07
800		2.75	2.12
815	2.58		2.18
835		3.01	2.27
840	3.20		2.29
850		3.21	2.34
865	2.83		2.40
875		3.00	2.45
890	2.98		2.52
900		3.49	2.56
915	3.05		2.63
925		3.32	2.67
945	3.20		2.76
950		3.78	2.78

* See Fig. 24.

the used MgO tubes. After obtaining these results, the use of MgO sheathing materials was discontinued, and other materials were investigated.

D. Conductivity Measurements Using Pyrolytic Boron Nitride

Since reproducible results could not be obtained using MgO tubes and MgO capillary sheathing materials, a pyrolytic boron nitride capillary (with a 0.76 mm I.D hole in the bottom of the tube) was used to sheath one of the platinum electrodes; the other electrode was left unsheathed. A cell constant of 49.7 cm^{-1} was determined using molten KCl at 800°C. The frequency dispersion of the resistance of molten $CaCl_2$ (Figure 25) showed that a frequency of at least ca. 10 kHz was needed to obtain the resistance independent of frequency; the measurements were, therefore, carried out at 20 kHz. The conductance of molten $CaCl_2$, shown in Figure 26 (points labeled ■), was observed to agree reasonably well with the recommended data (48) (Figure 26, line), although a difference in the slopes of the plots of κ with temperature was observed. After the addition of 2 mole percent CaO (Figure 26, points labeled *), the melt was allowed to remain at 800°C for 1 hour before its conductance was measured. After approximately 15 minutes, the resistance began to fluctuate in the range of ca. 30 ohms.

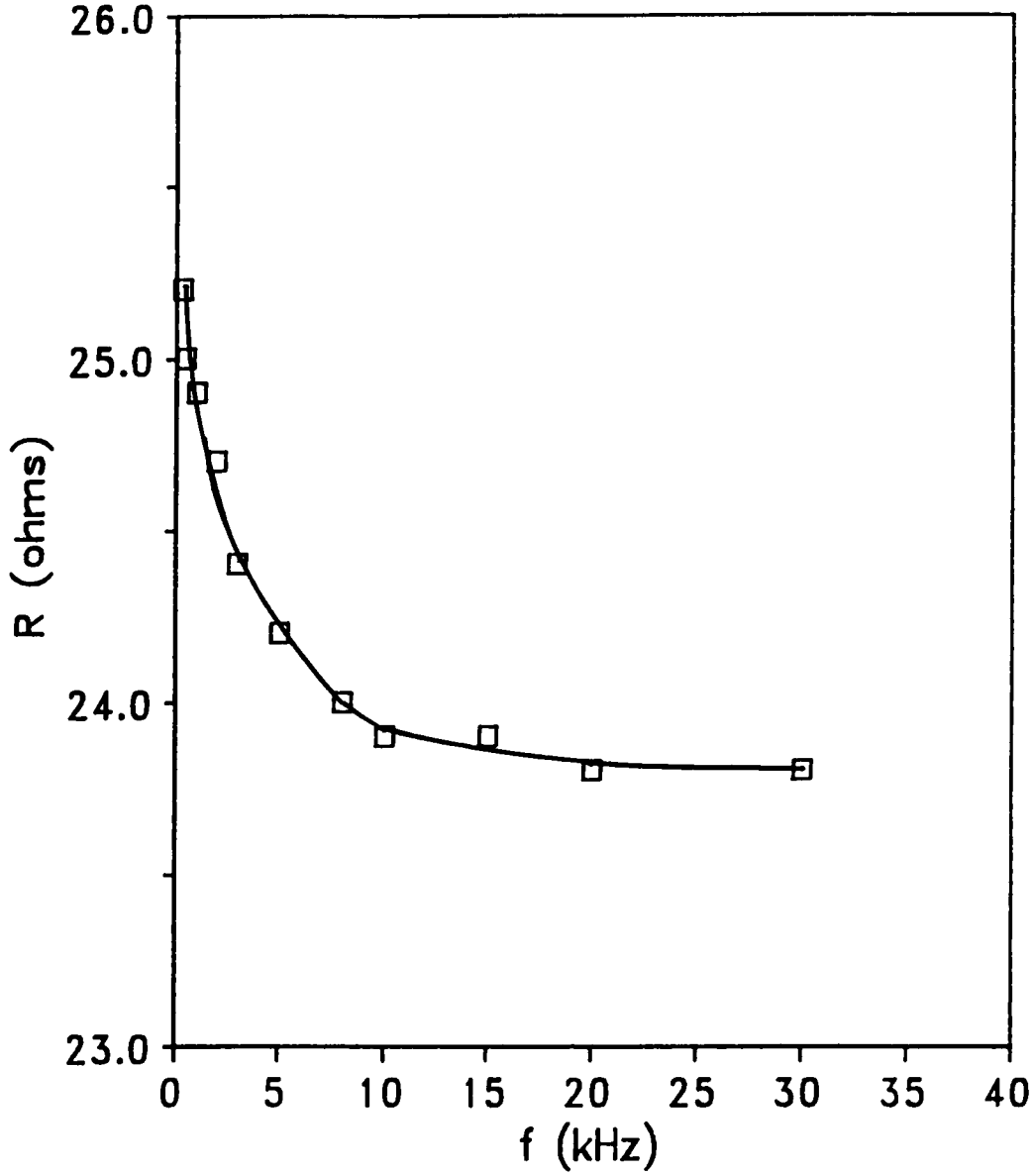


Figure 25. Frequency dispersion of the resistance of molten $CaCl_2$ at 800°C using a pyrolytic boron nitride capillary.

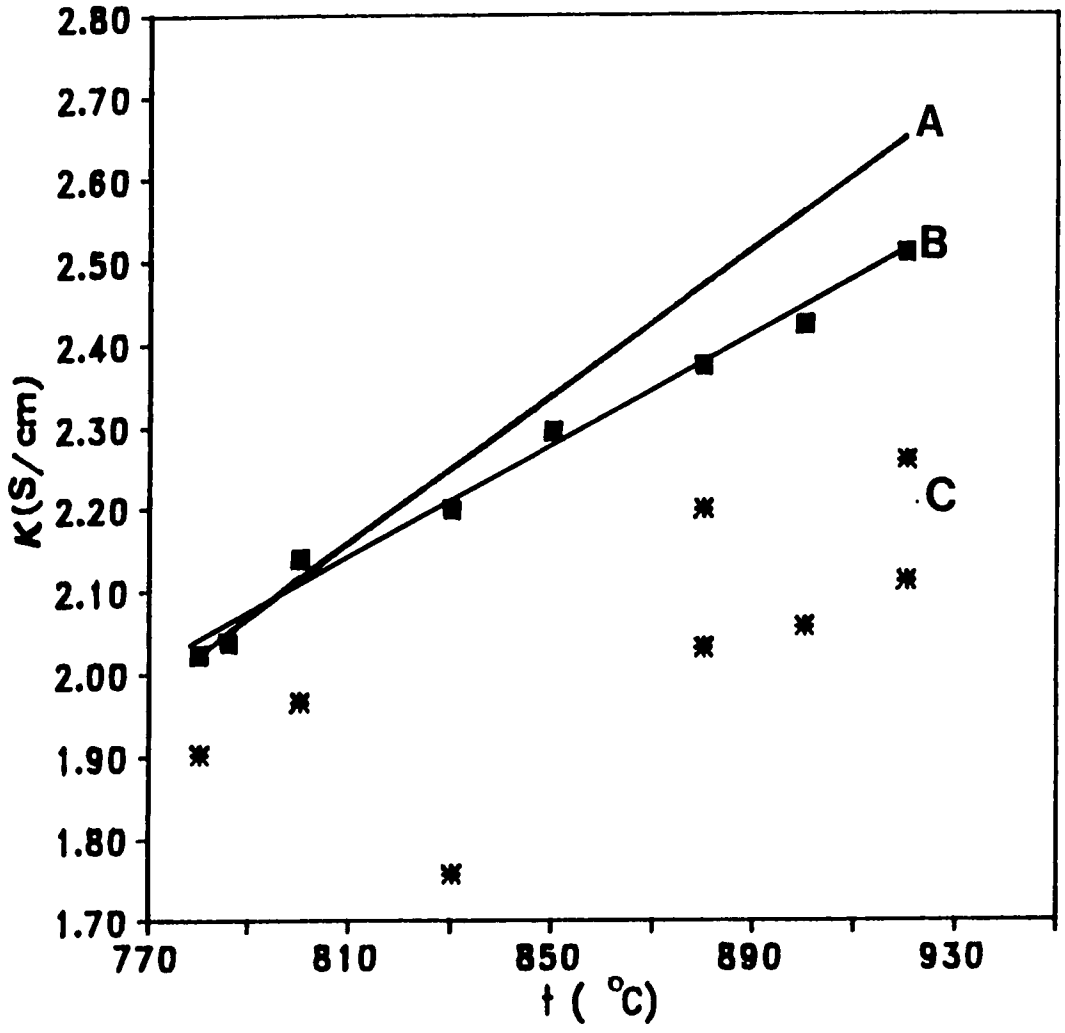


Figure 26. Specific conductivity data of: (A) recommended data for $CaCl_2$ (ref. 48); (B) molten $CaCl_2$; (C) molten $CaCl_2$-CaO (2 mole percent CaO).

After ca. 1 hour, the resistance became stable enough to measure the conductance at several temperatures; the data are summarized in Table 7. During the measurements, the resistance was observed to increase slowly, often increasing beyond the measuring capability of the bridge (100 kilo ohms). Movement of the cell consistently caused a sharp decrease in the measured resistance, followed by a gradual increase. The resistance values resulting from the movement of the cell were not constant. A second experiment (Figure 27, points labeled *) using the pyrolytic boron nitride capillary gave similar results. Upon the addition of CaO, the fluctuations in the measured resistance could not be stabilized; therefore, the conductance at several temperatures was not recorded. The results for molten $CaCl_2$ are summarized in Table 8. It is believed that the fluctuations in the resistance were due to the blocking of the capillary pin-hole, possibly by the undissolved CaO, since the dissolution of CaO in $CaCl_2$ has been shown to be slow (24). The thermodynamics of several reactions of boron nitride with the melt components was investigated, but none favored a reaction with the boron nitride. After the experiment, the cell constant was determined using molten KCl at 820°C, and was observed to decrease from 49.7 cm^{-1} to 48.3 cm^{-1}. It is believed that with the proper cell design,

Table 7

Specific Conductivity Data for a $CaCl_2$-CaO (2 mole % CaO) melt at 20 kHz using a pyrolytic boron nitride capillary

Temperature (°C)	Specific Conductivity (S/cm)		
	A*	B*	C*
780	2.03		1.90
790	2.05	2.04	
800	2.11	2.14	1.97
830	2.25	2.20	1.75
850	2.34	2.29	
880	2.47	2.37	2.03
900	2.56	2.42	2.06
920	2.65	2.51	2.11
780**	2.02	2.02	
880**	2.47		2.20
920**	2.65		2.26

* See Fig. 26.
**Returned to initial temperature.

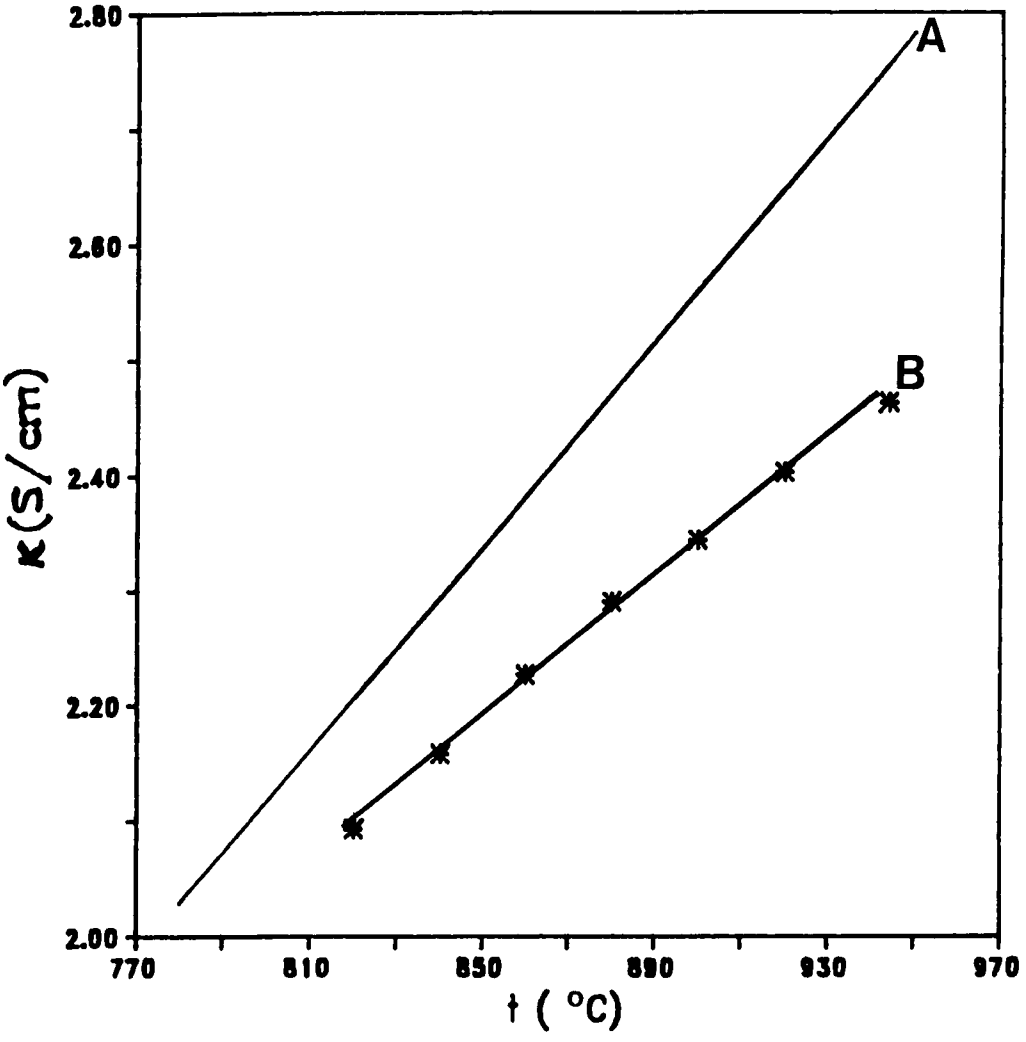


Figure 27. Specific conductivity data for molten $CaCl_2$: (A) recommended data (ref. 48); (B) measurements using a pyrolytic boron nitride capillary.

Table 8

Specific Conductivity Data for a $CaCl_2$ melt at 30 kHz using a pyrolytic boron nitride capillary

Temperature (°C)	Specific Conductivity (S/cm)	
	A*	B*
820	2.21	2.09
840	2.29	2.16
860	2.38	2.23
880	2.47	2.29
900	2.56	2.34
920	2.65	2.40
945	2.76	2.46
820**		2.09

* See Fig. 27.
** Returned to initial temperature.

pyrolytic boron nitride should be a suitable sheathing material for $CaCl_2$-CaO melts.

E. Other Materials Investigated

Additional materials were investigated for use as electrode sheathing material including zirconia, hot pressed boron nitride, and aluminum nitride.

Although zirconia (partially stabilized with Y_2O_3) did not appear to be attacked by a $CaCl_2$-CaO (12%) melt at ca. 900°C, it is known that the ionic conductivity of ZrO_2 is quite high above 800°C (92). This high conductivity may cause a short in the conducting path and result in incorrect conductance measurements.

Hot pressed boron nitride did not withstand the $CaCl_2$-CaO (14 mole %) melt at 900°C; its surface was pitted after the experiment.

Preliminary studies of aluminum nitride in the $CaCl_2$-CaO melt were promising. A compatibility study in a $CaCl_2$-CaO (14 mole %) melt at 900°C for 48 hours resulted in a 0.35% decrease in the weight of the aluminum nitride specimen; there was no apparent attack on the surface of the segment. This material may be useful for the $CaCl_2$-CaO melts.

CHAPTER 4

RESULTS AND DISCUSSION: ELECTROMOTIVE FORCE MEASUREMENTS OF $CaCl_2$-CaO MELTS

A. Selection of Reference Electrode

The silver-silver chloride reference electrode was chosen for use in the $CaCl_2$-CaO system for several reasons. Silver metal melts at 962°C; it exhibits only one common oxidation state, Ag(I). Silver chloride melts at 450°C and boils at 1550°C (92). Silver oxide decomposes at 230°C (93); the contamination of oxides on the surface of the metal, which is a serious problem in most systems, does not present a problem in the case of silver. Unlike some metals used for reference electrodes, silver metal was observed to be quite stable in a $CaCl_2$-CaO melt up to ca. 950°C. A disadvantage of the AgCl/Ag reference electrode is the continuous recrystallization of the silver metal when in contact with melts containing Ag^+. Recrystallization is due to the lateral migration of silver metal from hot zones to cool zones along the silver wire, and results in a wire eventually being converted into fragile loosely held joined crystals (94). This problem was minimized by using a small diameter (6 mm. O.D) quartz tubing to sheath the silver wire as shown in Figure 28.

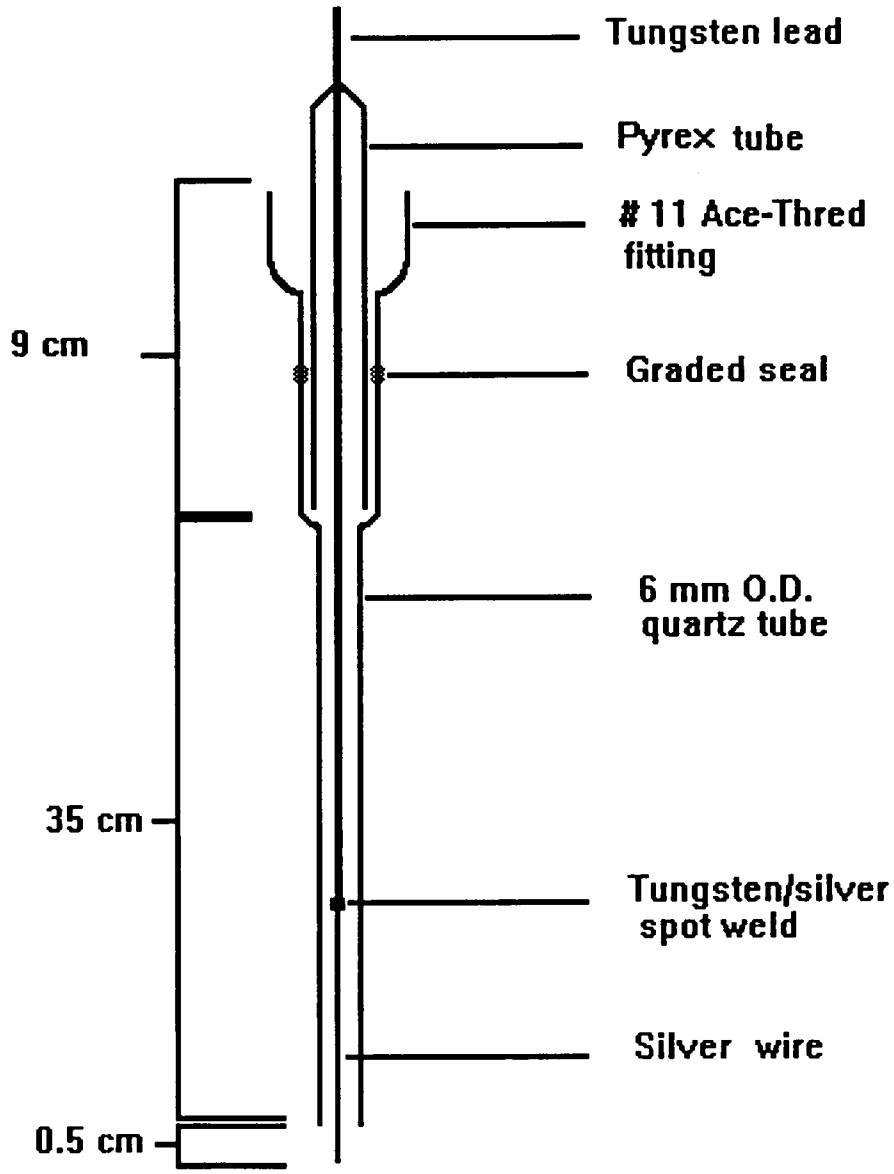


Figure 28. Sample half-cell electrode assembly.

B. Selection of a Reference Membrane

The selection of a reference half-cell membrane is dependent upon several criteria. A reference half-cell membrane must provide sufficient ionic conductivity and must be compatible with the melt of interest. The materials which were considered for reference half-cell membranes were limited due to the corrosive nature of CaO-containing melts and the high melting point of the $CaCl_2$-CaO melt (Figure 1, p. 4). Asbestos sealed in quartz (asbestos diaphragms) and Vycor glass were used as reference half-cell membranes, even though both were slowly attacked by the CaO-containing melt. A compatibility study showed that quartz and Vycor were completely attacked by a $CaCl_2$-CaO melt (12 mole %) after ca. 50 hours at 850°C. It was believed that this time was sufficient for obtaining emf data for several additions of AgCl. Vycor reference half-cell membranes were preferred because of their simpler construction and the elimination of possible leakage of the reference half-cell compartment. Although Vycor has a resistivity of ca. 20 x 10^6 ohm-cm at 800°C (95), its electrical conductivity at 800°C was sufficient to establish an electrical contact.

C. EMF Measurements

The applicability of the Nernst equation to the AgCl/Ag reference electrode in $CaCl_2$-AgCl and $CaCl_2$-CaO-AgCl melts was investigated. All of the data were corrected for a thermal potential, the potential due to the junction of two dissimilar metals (95), which was determined before each experiment after welding the ends of the silver wires and measuring the potential between 800°C and 950°C. Membrane potentials were determined during each experiment by adding the same AgCl concentration in both half-cells.

1. $CaCl_2$-AgCl System

Preliminary emf measurements were performed on the concentration cell

$$Ag/CaCl_2\text{-}AgCl(x_1=0.05)//asbestos//CaCl_2\text{-}AgCl(x_2=x)/Ag$$

where x_1 and x_2 are the mole fractions of AgCl. Electromotive force measurements were performed at 780°C, with x_2 ranging from 0.01 to 0.07 mole fraction. According to the Nernst equation (equation (11), p. 13) a plot of the measured emf versus log (Ag^+_s/Ag^+_r) should yield a straight line with a calculated slope of 2.303RT/F = 0.2089 at 780°C. The results of the measurements are shown in Figure 29, and are summarized in Table 9. The data were corrected for a

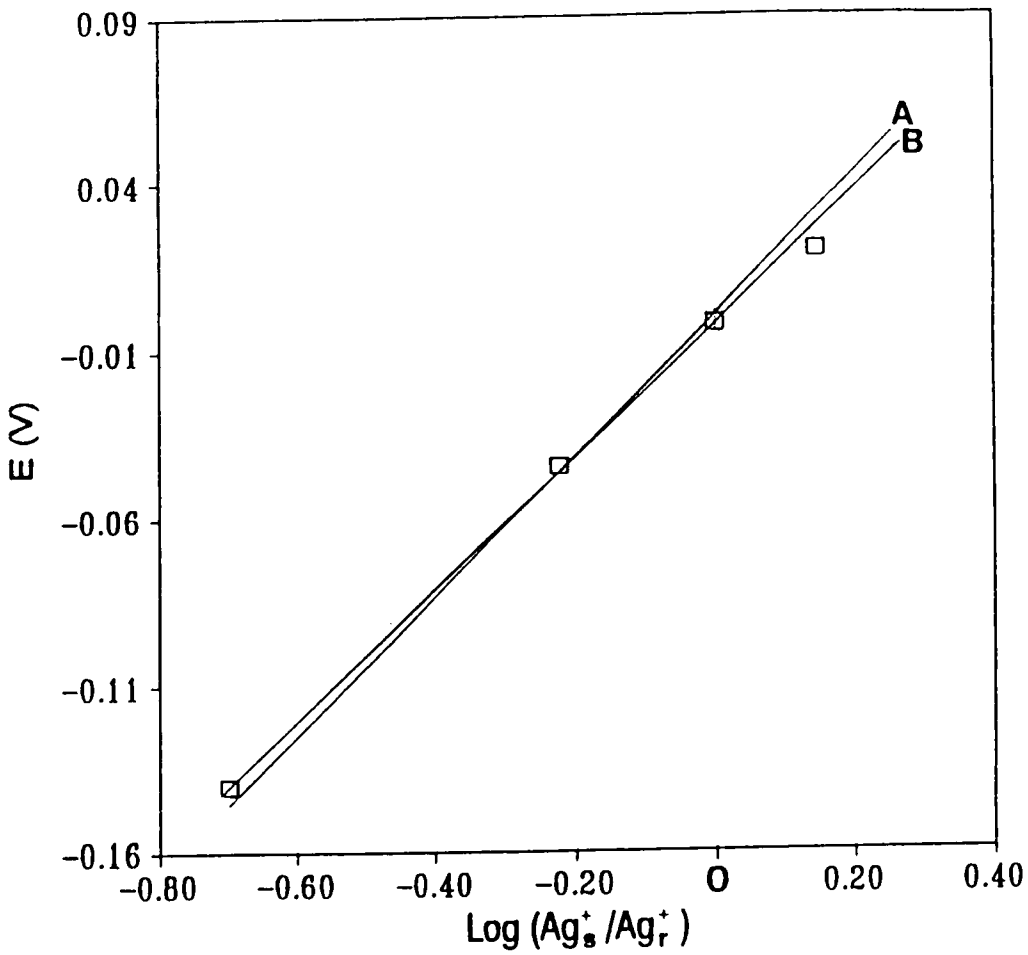


Figure 29. Nernst plot for a $CaCl_2$-AgCl melt using an asbestos reference half-cell membrane at 780°C: (A) calculated line; (B) measured data.

TABLE 9

Summary of emf data for a $CaCl_2$-AgCl melt at 780°C using an asbestos reference half-cell membrane

Ag(I), mole fraction	Log (Ag_s/Ag_r)	E (V)
0.010	-0.6990	-0.1405
0.030	-0.2218	-0.0450
0.050	0.0000	-0.0025
0.070	0.1461	0.0190

3 mV thermal potential. The data in Figure 29 were observed to exhibit Nernstian behavior with a slope of 0.1912, which deviated by 8.4% from the calculated slope of 0.2089. After an addition of AgCl, equilibrium was attained in 3 to 4 hours when the potential varied less than 0.3 mV for one hour. The absence of stirring was believed to have contributed to the long equilibration times. The stability of the reference electrode upon prolonged exposure to the melt was not studied, since it was known that the reference half-cell membrane would not endure the $CaCl_2$-CaO melt for more than ca. 50 hours.

Vycor glass was also used as a reference half-cell membrane for the concentration cell

$$Ag/CaCl_2\text{-}AgCl(x_1=0.05)//Vycor//CaCl_2\text{-}AgCl(x_2=x)/Ag$$

where x_2 ranged from 0.0100 mole fraction to 0.129 mole fraction. Although Vycor is similar to quartz in composition (96), it was preferred over asbestos diaphragms, due to the simpler construction of the reference half-cell. Figure 30 represents data collected for an emf experiment using a $CaCl_2$-AgCl melt at 810°C, and Table 10 summarizes the data. The slope of the line in Figure 30 is 0.2067, which deviates by 3.8% from the slope of the calculated line (0.2149). After an addition of AgCl, equilibrium was usually attained when the potential varied less than 0.3 mV

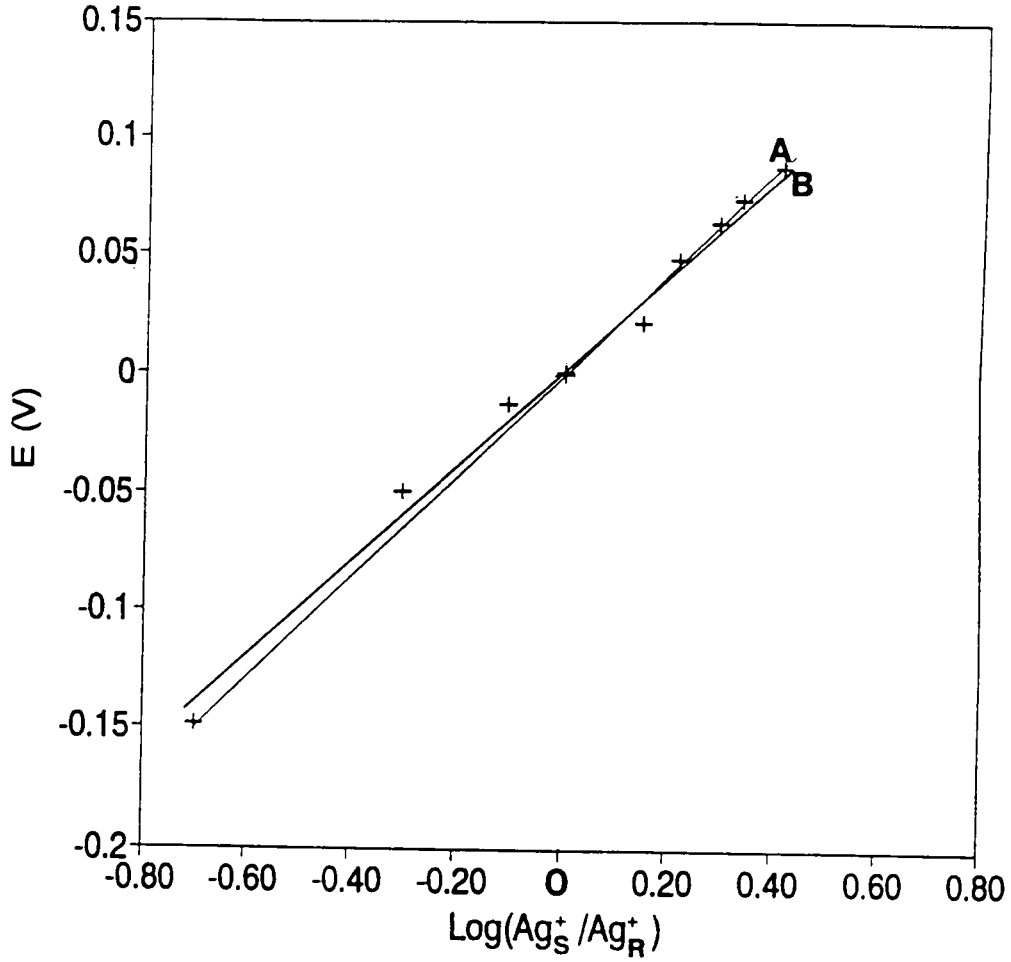


Figure 30. Nernst plot for a $CaCl_2$-AgCl melt at 810°C using a Vycor reference half-cell membrane: (A) calculated line; (B) measured data.

TABLE 10

Summary of emf data for a $CaCl_2$-AgCl melt at 810°C using a Vycor reference half-cell membrane

Ag(I), mole fraction	Log (Ag_s/Ag_r)	E (V)
0.010	-0.6990	-0.1455
0.025	-0.3010	-0.0465
0.039	-0.1079	-0.0095
0.050	0.0000	0.0042
0.070	0.1461	0.0250
0.082	0.2148	0.0512
0.096	0.2833	0.0662
0.109	0.3384	0.0760
0.129	0.4116	0.0904

for one hour, which typically took 4 to 6 hours. Figure 31 shows the effect of temperature on the emf which was determined by both increasing and decreasing the temperature in the range 810°C - 920°C. The emf of the cell for the AgCl composition of 0.08 mole fraction was observed to vary linearly with temperature with a slope of 2.8×10^{-5} V/deg, which deviated 31.7% from the calculated slope of 4.1×10^{-5} V/deg.

Since it was shown that the AgCl/Ag reference electrode performed reasonably satisfactorily and exhibited Nernstian behavior in $CaCl_2$-AgCl melts using both Vycor glass and asbestos diaphragms as reference half-cell membranes, Vycor reference half-cell membranes were examined in $CaCl_2$-CaO-AgCl melts.

2. $CaCl_2$-CaO-AgCl System

The applicability of the AgCl/Ag reference electrode in $CaCl_2$-CaO melts was investigated using the concentration cell

$$Ag/CaCl_2\text{-}AgCl(x_1=0.05)//Vycor//CaCl_2\text{-}CaO(x_2=0.03)\text{-}AgCl(x_3)/Ag$$

with the mole fraction x_3 ranging from 0.0100 to 0.118 at 820°C. The variation in the potential with time was not studied due to the attack on Vycor, resulting in experiments

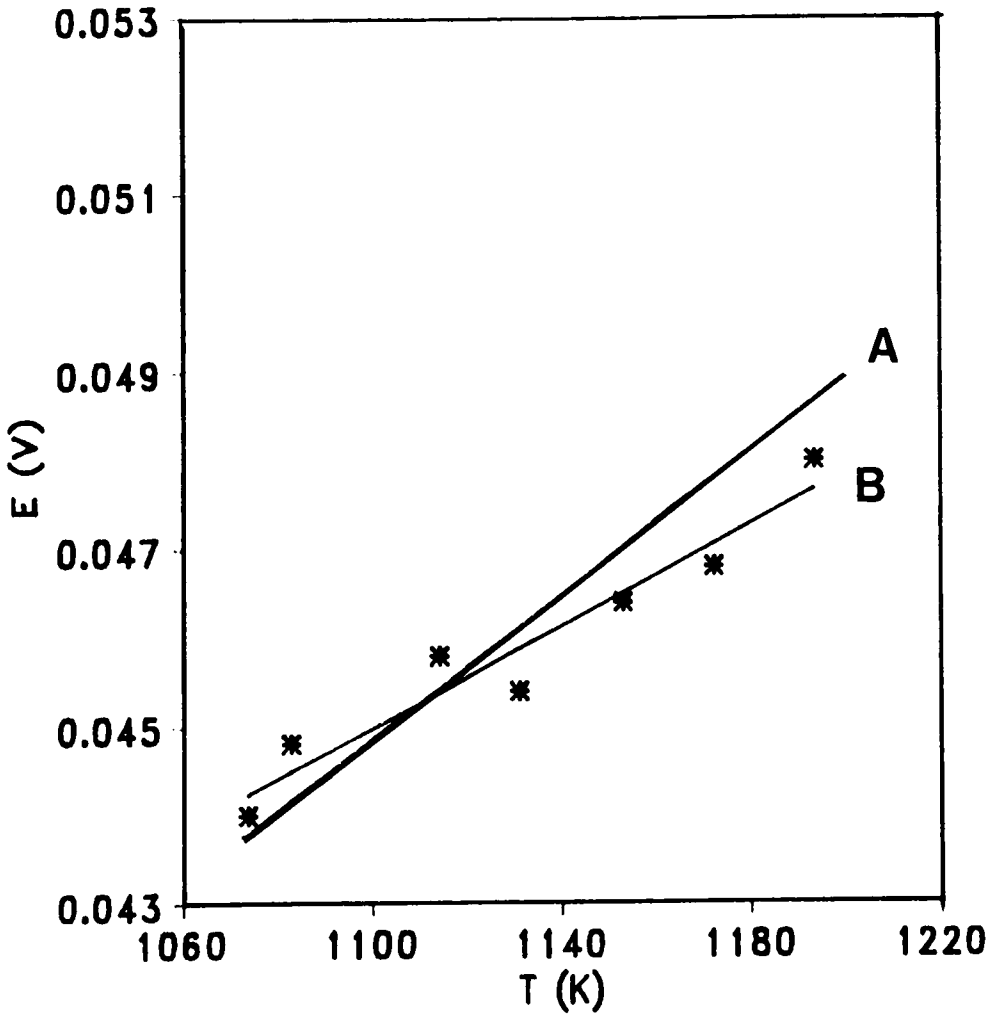


Figure 31. Variation of emf with temperature for a $CaCl_2$-AgCl melt using a Vycor reference half-cell membrane: (A) calculated line; (B) measured data.

lasting ca. 50 hours. Experiments were concluded when the reference half-cell membrane ruptured, resulting in the mixing of the half-cell compartments. Thus, a new reference electrode was used for each experiment. Thermal potentials were minimized by the extension of the silver wire into the Pyrex head of the cell (Figure 5, p. 32), where the silver/tungsten spot welds were approximately at room temperature; thermal potentials of < 0.1 mV were measured. Potentials were typically stable within six to eight hours for the initial composition and within approximately four hours for subsequent AgCl additions. It was therefore necessary to perform the experiments as quickly as possible to obtain a sufficient number of data points. Potentials were recorded for ca. 1 hour after equilibrium was attained.

Preliminary measurements performed on the concentration cell showed large negative deviations from the calculated data given by the Nernst equation (equation (11), p. 13). "Sponge-like" grayish deposits were observed on the bottom of the glassy carbon crucible. An experiment involving the addition of CaO to the $CaCl_2$-AgCl melt at 820°C resulted in a decrease in the measured potential. Figure 32 represents an experiment in which measurements were made at three AgCl concentrations (data points 1, 2, and 3, Fig. 32), before the addition of CaO (data point 4, Fig. 32). After the CaO addition, the potential was observed to decrease from 36 mV to 1 mV. A decrease in the potential of 2.73 mV was

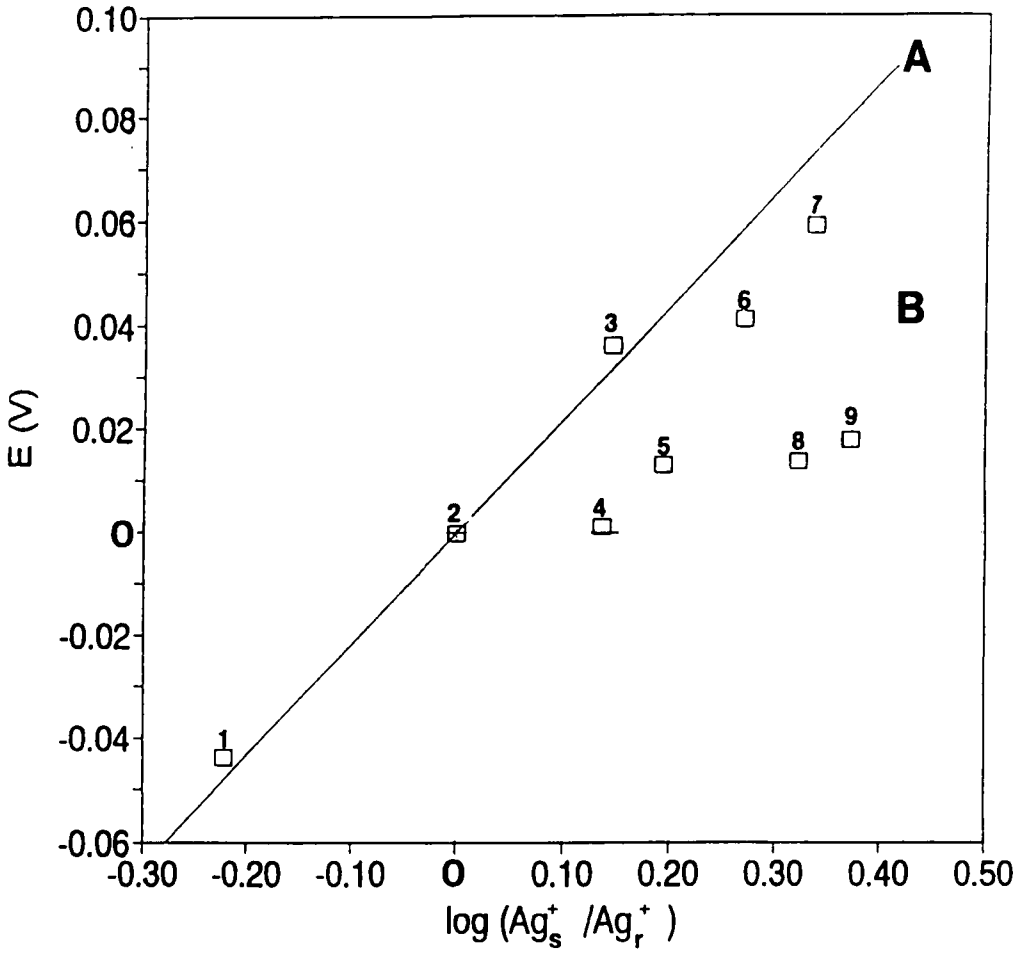


Figure 32. Nernst plot for a $CaCl_2$-CaO-AgCl melt at 820°C using a Vycor reference half-cell membrane: (A) calculated line; (B) measured data.

expected, due to the dilution of the melt from the added CaO. Upon subsequent additions of AgCl, potentials were observed to increase linearly (points 5-7, Fig. 32). Another addition of CaO (point 8, Fig. 32) showed a 45.4 mV decrease in the measured potential, and showed an increase upon the addition of AgCl. The data are summarized in Table 11. This experiment demonstrated that the potentials changed upon additions of CaO. Such changes could have been caused by a decrease in Ag^{+}_{s}, resulting in a decrease in the measured potential. After dismantling the cell, a "sponge-like" grayish deposit was again observed on the bottom of the crucible. From the thermodynamic data provided by Barin and Knacke (97), the free energy was determined for the reaction

$$2AgCl\ (l) + CaO\ (l) + C\ (s) \longrightarrow CaCl_2\ (l) + 2Ag\ (s) + CO\ (g)$$

where C (s) represents the glassy carbon crucible. The free energy (ΔG) for the reaction is -41.5 kcal/mole at 1100 K, thus favoring the formation of silver metal. X-ray diffraction analysis of the "sponge-like" deposit confirmed the formation of silver metal. Further data analysis showed that the emf corresponding to the mole fraction of AgCl calculated from the difference in the moles of added AgCl from the moles of added CaO agreed well with the calculated data. These results explained the decrease in the measured

TABLE 11

Summary of emf data for a $CaCl_2$-CaO-AgCl melt at 820°C using a Vycor reference half-cell membrane and a glassy carbon crucible

Ag(I), mole fraction	Log (Ag_s/Ag_r)	E (V)
0.030	-0.2218	-0.0440
0.050	0.0000	-0.0005
0.070	0.1461	0.0360
0.068	0.1335	0.0010
0.078	0.1931	0.0130
0.093	0.2695	0.0410
0.109	0.3384	0.0590
0.105	0.3222	0.0136
0.118	0.3729	0.0176

potential with the added CaO, and explained the observed deviations of the potentials for the preliminary measurements.

The glassy carbon crucible was then replaced with a MgO crucible. The free energy (ΔG) was determined for several reactions involving MgO with the components of the melt, but none favored the formation of silver metal. Two experiments were performed with CaO-containing melts at 820°C, and are summarized in Tables 12 and 13, respectively. In the first experiment (Figure 33 , points labeled ▲), the first three data points were recorded with no added CaO (points 1-3, Fig. 33; numbers above the symbols), and resulted in a slope of 0.1785. After an addition of 0.03 mole fraction CaO (point 4, Fig. 33), the emf was observed to decrease by 11 mV, which was 3 mV lower than the calculated. Upon subsequent additions of AgCl, a variation in the slope (0.1387 for points 4-6, Fig. 33) from the calculated slope of 0.2170 was observed. In the second experiment (Figure 33, points labeled □), emf measurements were made at AgCl concentrations in the range 0.030 - 0.096 mole fraction, and an initial CaO concentration of 0.05 mole fraction (data points 1-4, Fig. 33; numbers below the symbols). The data are in good agreement with the calculated values with a slope of 0.2099, which deviates 3.3% from a calculated slope of 0.2170. After the addition of 0.08 mole fraction CaO (data point 5, Fig. 33), the potential was monitored after

TABLE 12

Summary of emf data for a $CaCl_2$-CaO-AgCl melt at 820°C using a Vycor reference half-cell membrane and a MgO crucible: Experiment #1

Ag(I), mole fraction	Log (Ag_s/Ag_r)	E (V)
0.029	-0.2365	-0.0349
0.076	0.1818	0.0510
0.090	0.2552	0.0460
0.082	0.2175	0.0530
0.098	0.2922	0.0620
0.109	0.3384	0.0700
0.107	0.3304	0.0607

TABLE 13

Summary of emf data for a $CaCl_2$-CaO-AgCl melt at 820°C using a Vycor reference half-cell membrane and a MgO crucible: Experiment #2

Ag(I), mole fraction	Log (Ag_s/Ag_r)	E (V)
0.030	-0.2218	-0.0410
0.051	0.0086	0.0005
0.070	0.1461	0.0279
0.086	0.2350	0.0574
0.082	0.2175	0.0519
0.096	0.2815	0.0600

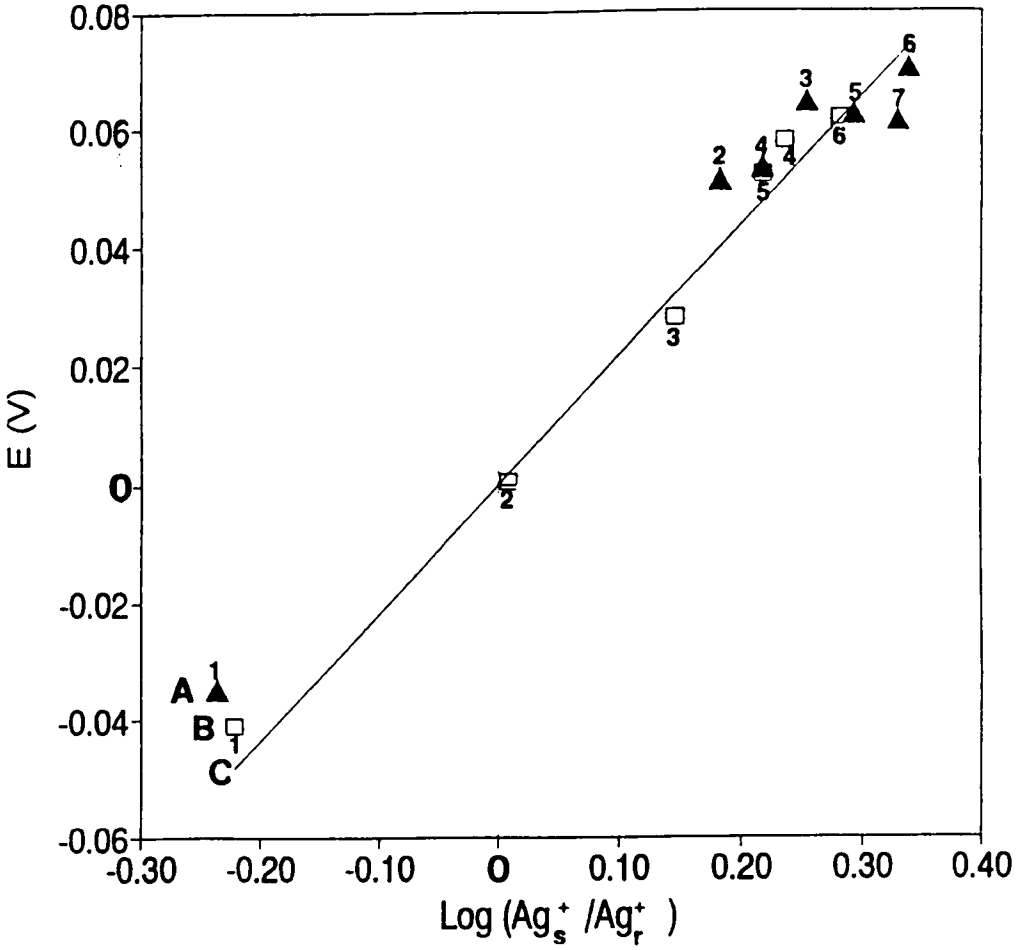


Figure 33. Nernst plot for $CaCl_2$-CaO-AgCl melts at 820°C using a Vycor reference half-cell membrane: (A) experiment #1 using a MgO crucible (▲); (B) experiment #2 using a MgO crucible (□); (C) calculated line.

allowing two hours for the CaO to dissolve in the melt, with the reference electrode elevated above the melt. This may have allowed sufficient time for the dissolution of the CaO in the melt, resulting in a lower deviation in the potential after an addition of CaO. Due to the degradation of the Vycor membrane, only one data point was obtained after the addition of CaO (0.08 mole fraction); a variation in slope compared to that of the calculated line could not be determined.

CHAPTER 5

SUMMARY

Selected electrochemical studies of $CaCl_2$-based melts were performed between the temperatures 790°C and 990°C. The conductivity of molten $CaCl_2$ using magnesia sheathing tubes was reproducible in the range 7 - 12%, and deviated 10 - 24% at 790°C and 990°C, respectively, from the recommended data (48). The reproducibility of the conductance isotherms for molten $CaCl_2$-CaO was poor; the results were not in agreement with previous results obtained by Flowers (91). Magnesia capillaries, although exhibiting a larger cell constant, gave results similar to those obtained with the magnesia tubes. The cell constant for both types of magnesia sheaths was observed to decrease with usage; this phenomenon was attributed to the attack on the magnesia sheaths by the melt. Arrhenius plots for the conductivity data of molten $CaCl_2$ and molten $CaCl_2$-CaO were observed to be linear with correlation coefficients of 0.99. Conductivity data for molten $CaCl_2$ using a pyrolytic boron nitride capillary were in reasonable agreement with the recommended data. Undissolved CaO in the $CaCl_2$ melt may have caused blockage of the pyrolytic boron nitride capillary, resulting in fluctuations in the measured resistance. It is believed that pyrolytic boron nitride may

be an adequate sheathing material for $CaCl_2$-CaO melts, provided the diameter of the capillary allows for sufficient mixing of the salts.

The utility of the AgCl/Ag reference electrode in $CaCl_2$-AgCl and in $CaCl_2$-CaO-AgCl melts, using asbestos diaphragms and Vycor glass as reference half-cell membranes, was also investigated. The reference electrode exhibited Nernstian behavior in $CaCl_2$-AgCl melts using an asbestos half-cell membrane and a Vycor membrane, with deviations in the slopes, of 8.3% and 3.8%, respectively, from the reported data. Upon additions of CaO to the $CaCl_2$-AgCl melt, potentials were observed to decrease; this effect resulted from the reduction of silver chloride by the glassy carbon crucible in the presence of CaO. Electromotive force data, collected using a Vycor reference half-cell membrane and a magnesia crucible, resulted in a 3.3% deviation in the slope from the reported data. Although further investigations are warranted, it is believed that the AgCl/Ag reference electrode will perform satisfactorily in the $CaCl_2$-CaO-AgCl melt, provided compatible materials are employed.

LIST OF REFERENCES

LIST OF REFERENCES

1. G. Mamantov, "Molten Salts: Characterization and Analysis," Marcel Dekker, New York (1969).

2. J. Braunstein, G. Mamantov, and G. P. Smith, "Advances in Molten Salt Chemistry," Vol. 1, Plenum Press, New York (1971).

3. J. Braunstein, G. Mamantov, and G. P. Smith,"Advances in Molten Salt Chemistry," Vol. 2, Plenum Press, New York (1973).

4. J. Braunstein, G. Mamantov, and G. P. Smith, "Advances in Molten Salt Chemistry," Vol. 3, Plenum Press, New York (1975).

5. J. Braunstein and G. Mamantov, "Advances in Molten Salt Chemistry," Vol. 4, Plenum Press, New York (1981).

6. G. Mamantov, "Advances in Molten Salt Chemistry," Vol. 5, Elsevier, Amsterdam (1983).

7. G. Mamantov, C. B. Mamantov, and J. Braunstein, "Advances in Molten Salt Chemistry," Vol. 6, Elsevier, Amsterdam (1987).

8. G. Mamantov, "Characterization of Solutes in Nonaqueous Solvents," Plenum Press, New York (1978).

9. B. R. Sundheim, "Fused Salts," McGraw-Hill, New York (1964).

10. D. G. Lovering and R. J. Gale, "Molten Salt Techniques," Vol. 1, Plenum Press, New York (1983).

11. D. G. Lovering and R. J. Gale, "Molten Salt Techniques," Vol. 2, Plenum Press, New York (1984).

12. D. G. Lovering and R. J. Gale, "Molten Salt Techniques," Vol. 3, Plenum Press, New York (1987).

13. M. Blander, "Molten Salt Chemistry," Interscience, New York (1964).

14. Iu. K. Delimarskii and B. F. Markov, "Electrochemistry of Fused Salts," Sigma Press, Washington, D.C. (1961).

15. D. Pletcher and F. C. Walsh, "Industrial Electrochemistry," p. 221, Chapman and Hall, New York (1990).

16. G. J. Janz, "Molten Salts Handbook," pp. 411-456, Academic Press, New York (1967).

17. F. Lantelme, A. Barhoun, and G. Li, J. Electrochem. Soc., **139**, 1249 (1992).

18. Cl. Decroly, A. Mukhtar, and R. Winand, J. Electrochem. Soc., **115**, 905 (1968).

19. J. C. Spirlet, J. R. Peterson, and L. B. Asprey, in "Advances in Inorganic Chemistry," H. J. Emeleus and A. G. Sharpe, eds., pp. 1-37, Academic Press, New York (1987).

20. L. J. Mullins, D. C. Christensen, and B. R. Babcock, "Fused Salt Processing of Impure Plutonium Dioxide to High-Purity Plutonium Metal," Los Alamos National Laboratory Report LA-9154-MS (1982).

21. W. Z. Wade and T. Wolf, J. Nucl. Sci. Tech., **6**, 402 (1969).

22. D. A. Wenz, I. Johnson, and R. D. Wolson, J. Chem. Eng. Data, **14**, 250 (1969).

23. M. S. Coops, J. B. Knighton, and L. J. Mullins, in "Plutonium Chemistry," Chapter 25, W. T. Carnall and G. R. Choppin, eds., ACS Symposium Series 216, American Chemical Society, Washington D.C. (1983).

24. G. S. Perry and L. G. MacDonald, J. Nucl. Mat., **130**, 234 (1985).

25. R. A. Sharma and R. N. Seefurth, J. Electrochem. Soc., **135**, 66 (1988).

26. J. L. Margrave and G. Mamantov, in "High Temperature Materials and Technology," I. E. Campbell and E. M. Sherwood, eds., p. 95, John Wiley and Sons, New York (1967).

27. V. Z. Grebenik and K. Ya. Grachev, J. Anal. Chem. USSR, **23**, 1398 (1968).

28. Ref 26, pp. 96-97.

29. J. A. Plambeck, "Encyclopedia of Electrochemistry of the Elements," Vol I , A. Bard, editor, Marcel Dekker, Inc., New York (1973).

30. G. Jones and B. C. Bradshaw, J. Am. Chem. Soc., **55**, 1780 (1933).

31. G. Jones and M. J. Prendergast, J. Am. Chem. Soc., **59**, 731 (1937).

32. H. C. Parker and E. W. Parker, J. Am. Chem. Soc., **46**, 312 (1924).

33. P. Saulnier, J. Soln. Chem., **8**, 835 (1979).

34. P. Saulnier and J. Barthel, J. Soln. Chem., **8**, 847 (1979).

35. J. G. Janz and R. P. T. Tomkins, J. Electrochem. Soc., **124**, 55C (1977).

36. G. D. Robbins, J. Electrochem. Soc., **116**, 813 (1969).

37. K. Matiasovsky, V. Danek, and B. Lillebuen, Electrochim. Acta, **17**, 463 (1972).

38. F. J. Holler and C. G. Enke, in "Laboratory Techniques in Electroanalytical Chemistry," P. T. Kissinger and W. R. Heineman, eds., pp. 235-266, Marcel Dekker, New York (1984).

39. D. C. Grahame, J. Am. Chem. Soc., **63**, 1207 (1941).

40. J. Braunstein and G. D. Robbins, J. Chem. Educ., **48**, 52 (1971).

41. G. D. Robbins and J. Braunstein, in "Molten Salts: Characterization and Analysis," G. Mamantov, editor, Marcel Dekker, New York (1969).

42. G. Jones and S. M. Christian, J. Am. Chem. Soc., **57**, 272 (1935).

43. F. S. Feates, D. J. G. Ives, and J. H. Pryor, J. Electrochem. Soc., **103**, 580 (1956).

44. R. P. T. Tomkins, G. J. Janz, and E. Andalaft, J. Electrochem. Soc., **117**, 906 (1970).

45. A. M. Feltham and M. Spiro, Chem. Rev., **71**, 177 (1971).

46. J. D. Edwards, C. S. Taylor, A. S. Russell, and L. F. Maranville, J. Electrochem. Soc., **99**, 527 (1952).

47. R.W. Laity in "Reference Electrodes," D. J. G. Ives and G. J. Janz, eds., pp. 548-558, Academic Press, New York (1961).

48. G. Janz, F. W. Dampier, G. R. Lakshminarayanan, P. K. Lorenz, and R. P. T. Tomkins, "Molten Salts: Volume 1, Electrical Conductance, Density, and Viscosity Data," National Standard Reference Data Series, National Bureau of Standards 15 (1968).

49. J. O'M. Bockris, E. H. Crook, H. Bloom, and N. E. Richards, Proc. R. Soc. London, Ser A, **255**, 558 (1960).

50. E. R. Van Artsdalen and I. S. Yaffe, J. Phys. Chem., **59**, 118 (1955).

51. E. K. Lee and E. P. Pearson, Trans. Electrochem. Soc., **88**, 171 (1945).

52. K. Grjotheim, R. Nikolic, and H. A. Oye, Acta Chem. Scand., **24**, 489 (1970).

53. G. J. Janz, "NIST Properties of Molten Salts Database," Version 1.0, MSDC-RPI, Rensselaer Polytechnic Institute, New York (1992).

54. Y. Iwadate, K. Igarashi, J. Mochinaga, and T. Adachi, J. Electrochem. Soc., **133**, 1162 (1986).

55. J. Mochinaga, Y. Iwadate, and K. Igarashi, J. Electrochem. Soc., **138**, 3588 (1991).

56. K. Fukushima, Y. Iwadate, Y. Andou, T. Kawashima, and J. Mochinaga, Z. Naturforsch, **46a**, 1055 (1991).

57. G. J. Janz, R. P. T. Tomkins, C. B. Allen, J. R. Downey, Jr., G. L. Gardner, U. Krebs, and S. K. Singer, J. Phys. Chem. Ref. Data, **4**, 871 (1975).

58. G. J. Janz, "NIST Properties of Molten Salts Database," Version 2.0, MSDC-RPI, Rensselaer Polytechnic Institute, New York (1992).

59. J. W. Tomlinson in "Physico-Chemical Measurements at High Temperatures", J. O'M Bockris, J. L. White, and J. D. MacKenzie, eds., p. 252, Butterworth Scientific Publishers, London (1959).

60. A. E. van Arkel, E. A. Flood, and N. Bright, Can. J. Chem., **31**, 1009 (1953).

61. T. Baak, Acta Chem. Scand., **8**, 1727 (1954).

62. T. Baak, Acta Chem. Scand., **9**, 1406 (1955).

63. J.O'M. Bockris, J. A. Kitchener, S. Ignatowicz, and J. W. Tomlinson, Disc. Faraday Soc., **4**, 265 (1948).

64. J.O'M. Bockris, J. A. Kitchener, S. Ignatowicz, and J. W. Tomlinson , Trans. Faraday Soc., **48**, 75 (1952).

65. A. E. Martin and G. Derge, Trans. Am. Inst. Min. Mater. and Eng., **154**, 104 (1943).

66. J. C. Nichol and R. M. Fuoss, J. Phys. Chem., **58**, 696 (1954).

67. M. Spiro, in "Physical Methods of Chemistry" Chapter 8, B. W. Rossiter and J. F. Hamilton, eds., John Wiley and Sons, New York (1986).

68. A. U. Seybolt and J. E. Burke, "Procedures in Experimental Metallurgy," p. 64, John Wiley and Sons, New York (1953).

69. K. W. Fung and G. Mamantov, in "Advances in Molten Salt Chemistry," Vol. 2, J. Braunstein, G. Mamantov, and G. P. Smith, eds., p. 227, Plenum Press, New York (1973).

70. C. H. Liu, K. E. Johnson, and H. A. Laitinen in "Molten Salt Chemistry,"M. Blander, editor, pp. 681-733, Interscience, New York (1964).

71. A. F. Alabyshev, M. F. Lantratov, and A. G. Morachevskii, "Reference Electrodes for Fused Salts," Sigma Press, Washington, D.C. (1965).

72 M. Bruneaux, J. Hladik, Y. Pointud, and G. Morand, Electrochim. Acta, **13**, 1591 (1968).

73. S. N. Flengas and T. R. Ingraham, J. Electrochem. Soc., **106**, 714 (1959).

74. S. N. Flengas and T. R. Ingraham, Can. J. Chem., **35**, 1139 (1957).

75. S. N. Flengas and T. R. Ingraham, Can. J. Chem., **36**, 780 (1958).

76. S. N. Flengas and T. R. Ingraham, Can. J. Chem., **36**, 1103 (1958).

77. P. J. Tumidajski and S. N. Flengas, J. Electrochem. Soc., **138**, 1659 (1991).

78. P. J. Tumidajski and S. N. Flengas, J. Electrochem. Soc., **137**, 2717 (1990).

79. L. Yang and R. G. Hudson, J. Electrochem. Soc., **106**, 986 (1959).

80. H. A. Laitinen and C. H. Liu, J. Am. Chem. Soc., **80**, 1015 (1958).

81. S. M. Selis and L. P. McGinnis, J. Electrochem. Soc., **108**, 191 (1961).

82. K. H. Stern, J. Phys. Chem., **60**, 679 (1956).

83. S. N. Flengas and E. Rideal, Proc. R. Soc. London, **233A**, 443 (1956).

84. R. Combes, J. Vedel, and B. Tremillon, Electrochim. Acta, **20**, 191 (1975).

85. R. J. Labrie and V. A. Lamb, J. Electrochem. Soc., **106**, 895 (1959).

86. R. Roumieu and A.D. Pelton, J. Electrochem. Soc., **128**, 50 (1981).

87. R. Littlewood, Electrochim. Acta, **3**, 270 (1961).

88. D. L. Maricle and D. N. Hume, J. Electrochem. Soc., **107**, 354 (1960).

89. L. E. Topol and S. J. Yosim, Synthesis in Inorganic and Metal-Organic Chemistry, **3**, 47 (1973).

90. D. F. Evans and M. A. Matesich, in "Techniques of Electrochemistry," Chapter 1, E. Yeager and A.J. Salkind, editors, John Wiley and Sons, New York (1973).

91. P. Flowers and G. Mamantov, "Investigations of Calcium Chloride-Based Molten Salt Systems," Final Report to Los Alamos National Laboratory (1989).

92. G. V. Samsonov, "The Oxide Handbook," Chapter 4, pp. 273-274, Plenum Press, New York (1973).

92. R. C. Weast, "Handbook of Chemistry and Physics," 66th ed., p. B-139, CRC Press, Boca Raton, Florida (1985).

93. Reference 92, p. B-140.

94. Reference 47, p. 589.

95. Reference 47, p. 583.

96. Reference 68, p. 66.

97. I. Barin and O. Knacke, Thermochemical Properties of Inorganic Substances, Springer-Verlag, New York (1973).

VITA

Thomas Paul Blanchard Jr., son of Thomas and Elaine Blanchard Sr., was born in Pierre Part, Louisiana on August 27, 1966. He graduated from Assumption High School in June of 1984 and subsequently entered Nicholls State University in Thibodaux, Louisiana, where he received the Bachelor of Science degree in Chemistry in December of 1988. In January of 1989, he entered the graduate program in chemistry at the University of Tennessee and received his Master of Science degree in Chemistry in December of 1992.